HHS Public Access

Author manuscript

Free Radic Biol Med. Author manuscript; available in PMC 2016 September 01.

Published in final edited form as:

Free Radic Biol Med. 2015 September ; 86: 90–101. doi:10.1016/j.freeradbiomed.2015.05.028.

Sulforaphane protects the heart from doxorubicin-induced toxicity

Preeti Singh[1,2], **Rajendra Sharma**[1], **Kevin McElhanon**[1,2], **Charles D. Allen**[1,2], **Judit K. Megyesi**[2,3], **Helen Beneš**[4], and **Sharda P. Singh**[1,2]

[1]University of Arkansas for Medical Sciences, Department of Pharmacology and Toxicology

[2]Central Arkansas Veterans Healthcare System, Little Rock, USA

[3]University of Arkansas for Medical Sciences, Department of Medicine

[4]University of Arkansas for Medical Sciences, Department of Neurobiology and Developmental Sciences

Abstract

Cardiotoxicity is one of the major side effects encountered during cancer chemotherapy with doxorubicin (DOX) and other anthracyclines. Previous studies have shown that oxidative stress caused by DOX is one of the primary mechanisms for its toxic effects on the heart. Since the redox-sensitive transcription factor, Nrf2, plays a major role in protecting cells from the toxic metabolites generated during oxidative stress, we examined the effects of the phytochemical sulforaphane (SFN), a potent Nrf2-activating agent, on DOX-induced cardiotoxicity. These studies were carried out both *in vitro* and *in vivo* using rat H9c2 cardiomyoblast cells and wild type 129/sv mice, and involved SFN pretreatment followed by SFN administration during DOX exposure. SFN treatment protected H9c2 cells from DOX cytotoxicity and also resulted in restored cardiac function and a significant reduction in DOX-induced cardiomyopathy and mortality in mice. Specificity of SFN induction of Nrf2 and protection of H9c2 cells was demonstrated in Nrf2 knockdown experiments. Cardiac accumulation of 4-hydroxynonenal (4-HNE) protein adducts, due to lipid peroxidation following DOX-induced oxidative stress, was significantly attenuated by SFN treatment. The respiratory function of cardiac mitochondria isolated from mice exposed to DOX alone was repressed, while SFN treatment with DOX significantly elevated mitochondrial respiratory complex activities. Co-administration of SFN reversed the DOX-associated reduction in nuclear Nrf2 binding activity and restored cardiac expression of Nrf2-regulated genes, at both the RNA and protein levels. Together, our results demonstrate for the first time that the Nrf2 inducer, SFN, has the potential to provide protection against DOX-mediated cardiotoxicity.

Author for correspondence: Sharda P. Singh, PhD, University of Arkansas for Medical Sciences, Department of Pharmacology and Toxicology, 4301 West Markham, Slot 638, Little Rock, AR 72205, Phone: 501-257-4806, ssingh@uams.edu.

Disclosures

No conflicts of interest, financial or otherwise, are declared by the author(s).

Graphical abstract

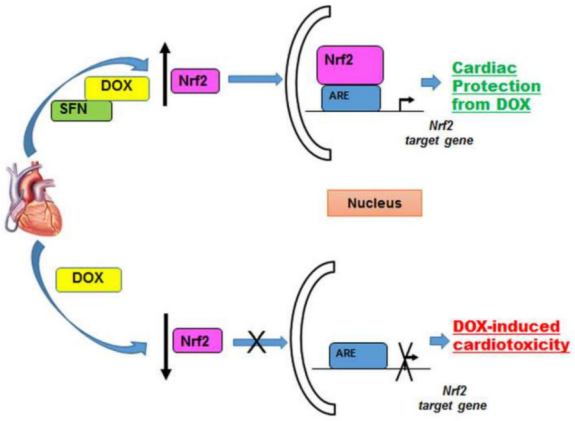

Keywords

Sulforaphane; Doxorubicin; *Nrf2*; Oxidative Stress; Cardiotoxicity; Cardiac Functions; Reactive oxygen species

Introduction

DOX is a highly effective anti-neoplastic agent widely in use to treat many cancer types [1, 2]. However, dose-dependent cardiotoxicity limits its long-term use in chemotherapy which strongly impacts the quality of life and survival of cancer patients [3-6]. Cardiotoxicity associated with DOX chemotherapy is estimated to afflict 10% to 25% of patients [7] and can develop immediately, within months, or even years after completion of therapy [8].

The mechanisms for DOX cardiotoxicity involve free radical-induced oxidative stress, production of reactive oxygen species (ROS) [9, 10] and in particular, mitochondrial dysfunction which can lead to cardiomyocyte apoptosis. Oxidative stress, lipid peroxidation, and production of lipid aldehydes are detected in cardiac tissues within three hours after DOX administration [3]. Tissues with abundant antioxidant enzymes are usually protected from oxidants produced by DOX. However, a high density of mitochondria and lower levels of ROS detoxification enzymes, as compared to other tissues, make the heart more susceptible to free radical damage and DOX toxicity [11, 12]. In contrast, it is generally accepted that mechanisms of antitumor action of DOX are distinct from those responsible for its cardiotoxicity. DOX antitumor activity is thought to be due to DNA damage and inhibition of cell replication in highly proliferative tumors. Intercalation of DOX into DNA and interference with DNA unwinding or DNA strand separation by inhibition of topoisomerase II are believed to result in apoptosis [13]. Cardiomyocytes are terminally differentiated cells with minimal replicative capacity and thus resistant to the antimitotic effects of DOX [14]. However, there are no targeted strategies to prevent DOX-induced cardiotoxicity; the resulting heart failure is treated after-the-fact by standard therapies to alleviate symptoms and limit further damage [15]. Clearly, devising a strategy to prevent DOX-induced cardiotoxicity would have tremendous benefit by limiting medical

complications and improving the quality of life. Several chemically and functionally diverse scavengers of ROS and lipid peroxidation products have been evaluated for their ability to mitigate DOX-induced cardiotoxicity, but with little success [5, 10, 16-18]. The major reasons for their lack of benefit may include: low bioavailability and/or low scavenging efficacy towards oxidants and electrophiles in a cellular system and/or secondary reactions with other biomolecules [19].

A central regulator of cellular responses to electrophilic/oxidative stress is the redox-sensitive transcription factor, Nrf2. Nrf2 is essential for detoxification gene activity [20] in mammalian cardiac cells [21-26]. Nrf2 accumulates in nuclei in response to oxidants and electrophiles, heterodimerizes with a small Maf protein, and activates the transcription of genes encoding enzymes (and other proteins) that are critical for the adaptation of cells to oxidative and electrophilic stress. Nrf2 binds to the antioxidant-responsive DNA elements or AREs found in the promoter regions of target genes [reviewed in 27]. Under physiological conditions, Nrf2 is bound in the cytosol by a repressor, the Kelch-like ECH associating protein 1 (Keap1). Keap1 functions as an adaptor for a Cullin 3 (Cul3)-based E3 ubiquitin ligase, a scaffold protein for the ubiquitination and degradation of Nrf2 [reviewed in 28]. Nrf2 is released from Keap1 in response to oxidative or electrophilic stress by modification of two critical cysteine residues [27] of Keap1 (C273 and C288) that are required for Keap1-dependent Nrf2 ubiquitination [29-31]. Since DOX alters mitochondrial functions in cardiac cells [32], protecting and enhancing the critical biological functions of Nrf2 should represent a safe and effective strategy to counter DOX toxicity during and after cancer treatment.

Sulforaphane (SFN), a phytochemical present in cruciferous vegetables, is a non-toxic compound recognized for its anti-cancer, anti-diabetic, antimicrobial and chemopreventive activity in different animal models of disease [33-36]. The major mechanism of chemopreventive action of SFN is considered to be the activation of Nrf2, via modification of cysteines of Keap1 [37, 38], resulting in transcriptional regulation of phase II detoxification and antioxidant genes through antioxidant response elements (AREs) in their promoters [reviewed in 39]. Enhanced Nrf2 signaling and cytoprotective gene activity induced by SFN were observed in cardiac cells *in vivo* [40, 41], in primary cardiomyocytes [42], and in the H9c2 cell line derived from rat atrial cardiomyoblasts [40]. Notably, SFN has not been tested for its ability to confer resistance to DOX toxicity or to other oxidative and electrophilic stresses on the heart *in vivo*. Hence, SFN-mediated activation of the Nrf2 pathway, upregulation of its target genes and subsequent activation of protective antioxidant and phase II enzymes, could offer an effective strategy to counter DOX-induced cardiomyopathy.

In this study, we examined the ability of SFN to protect against DOX-induced cardiotoxicity and analyzed the mechanisms of its protective role using cultured cardiomyoblasts (H9c2 cells) and a wild type (129/sv) mouse model. Results of these studies indicate that DOX is highly cytotoxic to H9c2 cells in a dose dependent manner which can be attenuated by SFN co-treatment with concomitant activation of Nrf2. Furthermore, our results demonstrate that SFN significantly prevented the development of DOX-induced cardiomyopathy *in vivo* via up-regulation of Nrf2 activity and via transcription of its target genes in the murine heart. Our study clearly establishes a basis for targeting Nrf2 as a therapeutic strategy to mitigate

DOX-induced cardiotoxicity and also to protect the heart from other forms of oxidative damage.

Materials and Methods

Reagents and Kits

DMEM cell culture medium, fetal bovine serum, Penicillin/streptomycin, phosphate buffered saline (PBS), 4% -12% Bis-TrisNuPAGE gels, running and transfer buffers, and SYBR green the QuantiTect Reverse Transcription Kit, the FastStart SYBR Green Master mix, the TransAM Nrf2 Kit, CytoTox 96® Non-Radioactive Cytotoxicity, OxiSelect™ Intracellular ROS Assay Kit (Green Fluorescence) Assay were purchased from Invitrogen/ Life Technologies (Grand Island, NY), Qiagen (Valencia, CA), Active Motif (Carlsbad, CA), Dojindo Molecular Technologies, Inc. (Rockville, MD), and Promega (Madison, WI), Cell Biolabs, Inc. (San Diego, CA), respectively. Primers for quantitative real-time PCR were synthesized by IDT (Coralville, IA, USA). All siRNA and DharmaFECT 1 transfection reagents were purchased from GE Dharmacon (Lafayette, CO). A monoclonal antibody against cytoplasmic actin (catalog number sc-8432) was purchased from Santa Cruz Biotechnology (Santa Cruz, CA). Polyclonal antibody against mGSTA4-4 was raised in chicken. All other primary and secondary antibodies used in this study were purchased from Santa Cruz Biotechnology, Inc. (Dallas, TX). All other reagents used in this study including sulforaphane, AMC and doxorubicin were purchased from Sigma (St. Louis, MO).

Cell Culture and Cell Viability Assay

The H9c2 cell line, derived from rat atrial cardiomyoblasts, was purchased from the American Type Culture Collection (ATCC; Manassas, VA) and maintained in high glucose DMEM (Dulbecco's Modification of Eagle's Medium), supplemented with 10% bovine calf serum and 1% penicillin–streptomycin solution at 37° C with 5% CO_2. Cultured adherent H9c2 cells were trypsinized and pelleted by centrifugation at 500×*g* for 5 minutes at 4°C and cells were washed twice by suspending in complete DMEM; cells were counted using a Z1 COULTER COUNTER® Cell and Particle Counter (Beckman Coulter Inc. Brea CA 92821). For cell viability assays, cell pellets were resuspended at 1×10^5 cells/ml in DMEM and 100 μL/well were seeded in 96-well plates and allowed to recover for 6-8 h before pretreatment with 2.5 μM SFN or vehicle for 12-14 h. Vehicle- or SFN-pretreated cells were subsequently treated with 5 μg/ml DOX or vehicle for an additional 16-18 h and analyzed for viability by the MTT assay using the CCK-8 kit (Dojindo, Rockville, Maryland) [43].

Nrf2 Knockdown and Cytotoxicity Assay

H9c2 cells (1×10^5) plated in 96-well plates were transfected with rat non-targeting siRNA (scrambled siRNA) or siRNA specific for rat *Nrf2* (25 nM final siRNA concentration) using DharmaFECT 1 Transfection Reagent, as per the manufacturer's instructions. After 48h of incubation at 37°C, cells were treated with SFN, DOX and SFN+DOX as described above and their viability was analyzed by using a CytoTox 96® Non-Radioactive Cytotoxicity Assay. Silencing of Nrf2 was confirmed by western blot analysis in a separate experiment.

Measurement of ROS Generation

For effects of SFN and/or DOX on ROS levels in H9c2 cells, 1×10^4 H9c2 cells were plated in growth medium and treated with SFN or DOX as described above. ROS production was measured in accordance with manufacturer's specifications using the OxiSelect™ Intracellular ROS Assay Kit (Green Fluorescence).

Caspase-3 Activation Assay

H9c2 cells (3×10^5) were plated in 100-mM dishes and allowed to recover for 6-8 h before pretreatment with 2.5 μM SFN or vehicle for 12-14 h. Vehicle- or SFN-pretreated cells were subsequently treated with 5 μg/ml DOX or vehicle for an additional 16-18 h. Cells were harvested and the pellets were washed in cold PBS twice. The washed cell pellets were lysed with 20 mM HEPES, pH 7.5, containing 10% sucrose, 0.1% CHAPS, 2 mM DTT, 0.1% NP40, 1 mM EDTA, 1 mM PMSF, 1μg/ml leupeptin and 1μg/ml pepstatin A at 4°C. The supernatants obtained were used to determine the activities of caspase-3 by a fluorometric assay using the amino-4-methyl coumarin (AMC)-tagged substrate DEVD (Asp-Glu-Val-Asp). In brief, protein extracts (50 μg protein) were incubated with 100 mM HEPES, pH 7.4, containing 10% sucrose, 0.1% CHAPS, 10 mM DTT and 50 μM of caspase substrate in a total reaction volume of 0.25 ml. After incubation for 60 min at 30°C, the amount of the liberated fluorescent group, AMC, was determined using a fluorescent spectrofluorometer (Perkin Elmer) with an excitation wavelength of 380 nm and an emission wavelength of 460 nm [44].

Animals and Treatment Plan

14 to 16 week-old male 129/sv mice were used to examine cardiac effects of SFN administration during chronic DOX treatment. All animal protocols were approved by the Institutional Animal Care and Use Committee of the Central Arkansas Veterans Healthcare System (CAVHS). Animals were housed in the Veterinary Medical Unit at the CAVHS in Little Rock, Arkansas (USA). A pilot study to establish the dose, frequency, and duration of SFN exposure required for Nrf2 activation and protection from DOX cardiotoxicity in wild type (WT, 129/sv) mice was performed and a dose of 4 mg/kg (*s.c.*) for 5 days/week of SFN treatment was found to be effective in cardio-protection. Mice were divided into four groups (control, SFN-, DOX- and SFN+DOX -treated mice). Two groups were injected with 4 mg/kg SFN or vehicle (PBS), 5 days/week for five weeks; this regimen provided one week of SFN pretreatment prior to DOX exposure. After one week of SFN or vehicle treatment, mice were injected with DOX (5 mg/kg) or vehicle once a week for the remaining four weeks (total of 20 mg/kg or 60 mg/mm^2). Mice were observed daily throughout the experiment for pain and distress by monitoring changes in grooming, mobility, food/water intake, and body weight. The survival experiment was done separately from all the others and all experiments were repeated to confirm the results as well as for statistical analyses.

Echocardiography

Transthoracic echocardiography was performed using the Vevo 770 high-resolution micro-imaging system (Visual Sonics, Toronto, Canada) fitted with an RMV 707-B Scan head (frequency 30 MHz, focal length 12.7 mm, frequency band 15–45 MHz) to assess cardiac

function [45]. Mice were anesthetized and maintained under 1-3% isoflurane during the procedure. Animals were mounted on a heated (37°C) platform; body temperature, breathing pattern, and heart rate were monitored during the echocardiogram recordings. Echocardiographic parameters were recorded at 350-420 beats/min, from at least three short-axis, M-mode recordings at the mid-left ventricle section of each mouse. Cardiac output was measured in the pulsed-wave Doppler mode. For the assessment of cardiac function, parameters were recorded at two time points: one day before starting treatments (for baseline values) and two days after the third DOX treatment.

Histopathology

Two days after final DOX injection, control and treated mice were euthanized and LV portions of the heart samples were fixed in 10% formalin followed by paraffin embedding, sectioning and staining of embedded tissue by routine procedures in the DNA Damage Core Facility at UAMS. Cardiac tissue was then evaluated for damage including myofibrillar disruption, fibrosis, and vacuolated pre-apoptotic cells. Disorganization of normal myofibrillar patterns (myofibrillar disruption) was scored for average severity (ranging from 1 to 3, least to most severe): 1, 1-2 foci or <10% of the total myocardium; 2, 10-30% of the total myocardium or focal lesions with extensive disruption; 3, >30% of total myocardium or multiple lesions with extensive disruption. Cytoplasmic vacuolization was also scored by severity (ranging from 1 to 3, least to most severe): 1, 1-3 myocytes; 2, 3-10 myocytes; or 3, >10 myocytes.

Determination of Cardiac Troponin-I Levels

Two days after the third DOX injection, blood was collected from the retro-orbital plexus of anesthetized mice using heparin-coated micro-hematocrit capillary tubes and MiniCollect® capillary blood collection tubes coated with EDTA (Greiner Bio-one, Monroe, NC). Plasma was separated from mouse blood by centrifuging whole blood for 10 min at 1,000*g*; the supernatant was isolated and centrifuged again at 10,000*g* for 5 min. If not used immediately, plasma samples were quick-frozen in liquid nitrogen and stored at −80°C until use. Briefly, a mouse cardiac troponin-I (cTn-I) ELISA kit from Life Diagnostics, Inc. (West Chester, PA) was used to assess troponin levels in 100 μl of plasma. The plasma was diluted three fold with the plasma diluent provided in the kit and assayed according to the manufacturer's protocol.

Body and Organ Weights

Body weights of control and treated mice were recorded once a week. A two-tailed *t*-test was used to analyze baseline-corrected body weight for significant differences between DOX-, SFN-, SFN+DOX- and PBS-treated groups and *p* values less than 0.05 were considered significant. Similarly, the effects of treatments on different organs (heart, lung, spleen and liver) of control and treated mice were assessed by organ weights at the time of animal euthanasia.

Determination of 4-HNE-Adduct Levels

4-hydroxynonenal (4-HNE) is an electrophilic, α,β-unsaturated lipid peroxidation product that accumulates with oxidative stress and is highly reactive, forming protein and DNA adducts [46]. A portion of left-ventricular (LV) cardiac tissue harvested from control and treated groups of mice was quick-frozen in liquid nitrogen and stored at −75°C until use. 4-HNE-adduct levels in LV samples were determined using an ELISA assay as previously described [47, 48]. In brief, a 20% (w/v) tissue homogenate was prepared in PBS containing a protease and phosphatase inhibitor mixture from Roche Diagnostics Corporation (Indianapolis, IN) [48]. The homogenates were sonicated for 10 sec at the lowest frequency and centrifuged at 3,000*g* for 15 min; the clear supernatant was collected and the protein level was measured using the Pierce 660nm Protein Assay (Thermo Scientific, Rockford, IL) reagent. 75 μg of protein was used for each determination.

High Resolution Respirometry

50 mg of myocardial tissue were freshly isolated from the left ventricles of control and treated mice and dissected in relaxing solution on ice to prepare fiber bundles as described previously [49, 50]. Myocardial fibers were permeabilized by gentle agitation in relaxing solution supplemented with 50 mg/ml saponin for 20 min at 4°C. Following washing in ice-cold respiration medium [51] for 10 min, fibers were maintained in this medium until the respirometric assay. Mitochondrial complex activities were measured at 37°C by the high resolution respirometry (HRR) technique using a substrate inhibitor titration protocol on an Oxygraph (Oroboros Instruments, Innsbruck, Austria). Complex I activity was tested by addition of the substrates, malate (2 mM) and glutamate (10 mM), to initiate respiration. To achieve maximal active respiration, 2.5 mM ADP was added, followed by inhibition of complex I respiration by addition of 0.1 μM rotenone. Complex II/III respiration was stimulated by addition of 10 mM succinate followed by addition of the complex III inhibitor antimycin A (10 μM). Lastly, complex IV respiration was measured by addition of 1μM N,N,N9,N9-Tetramethyl-p-phenylenediamine (TMPD) made in 0.8 M ascorbate (pH=6.0); complex IV activity was inhibited by adding 800 mM sodium azide. Data acquisition and analysis were performed using the DATLAB 4.2 software (Oroboros Instruments). Respiratory rates were expressed per milligram of dry weight.

Measurement of Active Nrf2 Binding

For western blot analysis and nuclear Nrf2 binding assays, 2.0×10^6 H9c2 cells were plated in 100-mm tissue culture dishes and treated as described above. After treatment, cells were harvested and cell nuclei were prepared for Nrf2 activity/binding assays and cell lysates for western blot analysis. Nuclear extracts were also prepared from the left ventricular (LV) portion of the heart isolated from vehicle- or DOX- with or without SFN-treated mice using the Nuclear Extract Kit (Active Motif, Carlsbad, CA) and stored at −80°C. Previously prepared nuclear extracts were tested for cytosolic and mitochondrial protein contamination by western blotting using antibodies against cytoplasmic actin and COX IV (abcam, Cambridge, MA), respectively. Within the detection limits of the method, no cytosolic or mitochondrial contamination was detected in nuclei prepared from heart tissue and H9c2

cells. Nuclear extracts (10-12 μg protein/sample) were assayed for Nrf2 binding activity, as previously described [45, 52], using the TransAMNrf2 Kit.

Determination of mRNA Levels by Real-Time Polymerase Chain Reaction

Total RNA was isolated from ventricular heart samples of control and treated mice by the guanidinium thiocyanate method, using the Fast RNA pro Green kit from MP Biomedicals (Solon, OH). Complementary DNA was prepared using the cDNA synthesis kit. In brief, 1 μg of RNA was mixed with anchored oligo-dT and random hexamers (1:1 ratio) and incubated at 42°C for 30 min; the reaction was stopped by bringing the temperature to 95°C for two min. Real-time polymerase chain reactions (qPCR) were performed in replicate on a DNA Engine Opticon 2 Detection System (MJ Research, Waltham, MA) with the SYBR green Master mix in a total volume of 20 μl containing 0.3 μM gene-specific primers. The cycling protocol was an initial denaturation at 95°C, followed by 40 cycles at 60°C. As previously reported [52, 53], the ribosomal protein S3 (RPS3) transcript was used as a reference for normalization of mRNA levels. Gene expression levels were normalized by calculating for each individual animal the difference, ΔCt, between S3 and the gene of interest. The average ΔCt for each replicate was exponentially transformed to obtain the expression level ($2^{-\Delta Ct}$) for each animal before determining the mean and standard deviation (n=5) for each treatment group.

Determination of Antioxidant/Anti-Electrophile Protein Levels by Western Blot Analysis

25 μg of heart tissue homogenate, obtained as described above, were resolved by SDS-PAGE in precast NuPage 4% - 12% Bis-Tris gels using MES running buffer (Invitrogen, Carlsbad, CA). The nitrocellulose membrane electroblot of the gel was probed with polyclonal antibodies against GSTA4-4[54], HO1, NQO1, SOD2 and Actin. A peroxidase-coupled secondary antibody and Super Signal Femto (Thermo Scientific, Rockford, IL) with chemiluminescent detection were used for visualization of bands on a Bio-Rad imaging system (Bio-Rad Laboratories, Hercules, CA).

Statistical Analysis

Statistical analyses were performed using GraphPad Prism Software version 6 (GraphPad Software Inc, La Jolla, CA). Two-tailed Students *t* tests were performed for all comparisons. Statistical significance was set at $p < 0.05$; results are expressed as the mean ± standard deviation. Survival curves were analyzed by the Log-rank (Mantel-Cox) test and Cox regression (for hazard ratios) was used for multivariate analysis (for hazard of dying).

Results

SFN-treated H9c2 cells are resistant to DOX toxicity

SFN is an electrophile capable of inducing expression of endogenous antioxidant and phase II enzymes through Nrf2-mediated transcription [37, 55-57]. DOX increases the production of ROS in cardiac myocytes, resulting in inflammation, apoptotic cell death and vacuolization [58]. Here we determined if the sensitivity of cardiac H9c2 cells to DOX toxicity could be attenuated by pretreatment of cells with SFN, and whether this SFN protection from DOX toxicity would be Nrf2-dependent. We first compared the effect of

DOX and SFN on the viability of H9c2 cells (data not shown). These studies indicated that DOX is highly toxic to these cells in a dose-dependent manner with an IC_{50} of 6.4 mg/ml. On the other hand, the $IC_{50}$of SFN was found to be 46.5 μM which is significantly higher than the concentration of 2.5 μM used to evaluate its protective effects described below. Next we analyzed whether or not SFN can confer protection against DOX-induced toxicity *in vitro*. We treated H9c2 cells with DOX, SFN or SFN+DOX for 24 h and assayed for cell viability. Results of these experiments showed that while DOX alone exhibited toxicity (showing less than 45% of cell viability at 5 μg/ml), co-treatment of H9c2 cells with SFN (2.5 μM) and DOX (5 μg/ml) resulted in significant protection of H9c2 cells (~76% cells were viable) against DOX-induced toxicity (Fig. 1A). These results formed the basis for further *in vivo* studies to determine whether pretreatment of WT mice with SFN could protect against DOX-induced cardiotoxicity through the activation of Nrf2 and the associated up-regulation of antioxidant and anti-electrophilic enzymes.

SFN inhibits DOX-induced activation of caspase-3 in H9c2 cells

Activation of caspase-3 due to DOX-toxicity is the hallmark of apoptosis in mammalian cardiac cells [59, 60]. In order to analyze the protective effect of SFN on DOX-induced apoptosis, we compared the activity of caspase-3 in SFN-, DOX- and SFN+DOX-treated H9c2 cells. Results presented in Fig. 1B indicated that DOX (5 μg/ml) treatment leads to high activation of caspase-3 activity in H9c2 cells which was significantly inhibited (>60%) by co-treatment with SFN (2.5 μM) and DOX, suggesting that SFN protected cells from DOX-induced apoptosis.

SFN-treated H9c2 cells are resistant to DOX toxicity in an Nrf2-dependent manner

Our earlier studies using the *mGSTA4*-null mouse model suggested a Nrf2-dependent protection against DOX toxicity [45]. We further determined whether or not SFN can confer protection, as described in Fig. 1A, of H9c2 cells against DOX-induced toxicity in an Nrf2-dependent manner *in vitro*. We silenced the expression of Nrf2 in H9C2 cells using Nrf2-siRNA while control cells were treated with scrambled (non-targeting) siRNA. After confirming the silencing of Nrf2 by western blot analysis (data not shown), cells were treated with SFN, DOX and DOX+SFN. The viability of control and treated cells was analyzed by an LDH release assay. We treated Nrf2-knockdown (KD) or control H9c2 cells with DOX, SFN or SFN+DOX as explained in the Methods section and assayed for cell viability. Results of these experiments showed that while DOX alone was toxic (showing less than 45% of cell viability at 5 μg/ml), co-treatment of H9c2 cells (scrambled siRNA-treated) with SFN (2.5 μM) and DOX (5 μg/ml) resulted in significant protection of H9c2 cells (>76% cells were viable) from DOX-induced toxicity (Fig. 2). Nrf2 KD itself affected transient viability of cells; but DOX treatment showed a worse effect on cell survival (~20% cell were viable) and even SFN treatment could not protect Nrf2 KD cells from DOX toxicity. Findings from this study clearly suggest that SFN protection from DOX toxicity is significantly Nrf2-dependent. These results formed the basis for further *in vivo* studies to determine whether pretreatment of WT mice with SFN could protect against DOX-induced cardiotoxicity through the activation of Nrf2 and the associated up-regulation of antioxidant and anti-electrophilic enzymes.

SFN efficiently blocks DOX-induced generation of ROS

It is well established that DOX treatment of cells and tissues causes generation of ROS [10] which contributes to DOX toxicity in both normal and cancer cells. To determine whether or not SFN could inhibit the DOX-induced generation of ROS in cardiac cells, we compared the generation of ROS in SFN-, DOX- and SFN+DOX-treated H9c2 cells. Results of these studies (Fig. 3) showed that SFN could significantly block (>60%) DOX-induced formation of ROS in cardiomyocytes.

SFN protects against DOX-induced cardiomyopathy

To examine if SFN provides cardioprotection during chronic DOX treatment *in vivo*, wild-type 129/sv mice were treated with SFN±DOX as described in the Materials and methods. A standard histological analysis of left ventricular tissue revealed increased pathology (cytoplasmic vacuolization, myofibrillar disruption and fibrosis) in DOX-treated mice as compared to SFN+DOX-treated mice (Fig. 4 and Table 1), indicating that SFN-treated mice exhibited resistance to DOX cardiomyopathy. Vehicle- or SFN-treated mice exhibited no cardiac pathology, whereas fibrosis was only observed in DOX-treated mice. In a similar experiment, cardiac function was assessed by echocardiography before DOX treatment and after the third DOX treatment. Cardiac ejection fraction (EF), fractional shortening (FS) and stroke volume (SV) parameters were essentially normal in the SFN+DOX-treated group. In contrast, mice treated with DOX alone exhibited impaired cardiac function (Fig. 5). In another 7-week survival experiment, only 8% of the mice treated with DOX alone survived, compared with a 75% survival fraction for SFN+DOX treated animals (Fig. 6). Comparison of DOX+SFN vs. DOX treatment alone, by a log-rank test, showed a significant difference in mortality rates ($p = 0.033$); Cox regression analysis indicated that SFN+DOX-treated mice had a 90% reduction in hazard of dying from DOX exposure compared to DOX-only treated mice.

SFN inhibits the DOX-mediated increase in cardiac troponin levels

Plasma levels of cardiac troponin T (cTnT) and cardiac troponin I (cTnI) are well established in clinical practice for assessing cardiac cell damage in cancer patients receiving DOX therapy [61]. Increase in cTnT and cTnI during DOX therapy reflects cardiac damage and indicates irreversible cardiomyocyte necrosis [61-64]. To access the effect of SFN during DOX therapy, we assayed cTnI levels in plasma from control and treated groups of mice. Average cTnI concentrations were significantly higher in all DOX-treated mice compared to SFN-, SFN+DOX- or vehicle-treated control mice (Fig. 7).

SFN prevents changes in body and organ weights caused by DOX

Body weights of control and treated mice were assessed after baseline (week 0) normalization of data for each animal in the control and treatment groups. Results showed a significant weight loss in the DOX-treated group, while SFN treatment reduced weight loss during DOX treatment and brought body weight close to the baseline weight. SFN- or vehicle-treated animals showed an insignificant increase in their body weights (Fig. 8A). Similarly, the effect of treatments on organ weights (heart, lung, spleen and liver) of control and treated mice was measured at the time of euthanasia. DOX-treated animals registered

lower weights of heart, lung and liver when compared with SFN+DOX or control animals (data not shown); but these changes did not meet the criteria of statistical significance ($p < 0.05$). However, spleen weights were significantly higher in DOX-treated animals compared with controls (Fig. 8B); and SFN co-treatment during DOX therapy maintained the spleen weight close to that of control animals. Increase in spleen weight, as reported earlier [61], could be because of gross lesions and increase in hematopoietic cell proliferation in the tissue during the DOX therapy.

SFN treatment reduces the DOX-induced formation of 4-HNE adducts in cardiac tissues

DOX treatment enhances production of the highly reactive lipid peroxidation product HNE in cardiac tissue [65, 66] and forms 4-HNE-protein adducts after interaction with lysine, histidine, and cysteine residues of proteins and peptides. 4-HNE-protein adducts modify protein functions and keep accumulating at high levels in tissues under oxidative/electrophilic stress [3]. To determine if SFN countered 4-HNE-adduct formation during DOX therapy, we examined the levels of 4-HNE-protein adducts. Results of these analyses (Fig. 9) revealed that the level of 4-HNE-protein adducts was significantly higher in the hearts of DOX-only treated animals. SFN treatment reduced HNE-adduct formation in the hearts of DOX-treated animals, with adduct levels remaining close to those of the control group.

SFN improves mitochondrial function during DOX treatment

DOX metabolism in cardiac cells involves its conversion into a more reactive semiquinone by the mitochondrial complex I of the electron transport chain (ETC), resulting in increased oxidative stress [64, 67]. Pharmacological activation of Nrf2 by SFN should remove excess ROS produced during DOX therapy by elevation of phase II detoxification and antioxidant enzyme activities and preserve ETC complex function. To evaluate changes in the ETC, its activity was measured in left ventricular biopsies of SFN- and/or DOX-treated mice (and controls) by high resolution respirometry (HRR) as described in the Materials and methods [51]. Results of these studies clearly revealed that DOX treatment significantly repressed complex I, II+III and IV activities. However, SFN restored these functions in the SFN +DOX-treated group (Fig. 10). Interestingly, we did not observe any significant changes in the activities of the various complexes in the SFN-only treated group.

Nrf2 is activated in SFN-treated H9c2 cells and in hearts of treated mice

The chronic response to DOX-induced myocardial injury involves increased oxidative and electrophilic stress [24, 68]. The enhanced survival of H9c2 cells (Fig. 1) and animals (Fig. 6), and the return to normal cardiac function following SFN pretreatment and co-treatment with DOX (Fig. 5) suggested activation of a protective mechanism in the heart. SFN is known to facilitate nuclear translocation of Nrf2, to induce stress-responsive gene expression and to upregulate anti-oxidative and anti-electrophile defenses [69, 70]. Therefore, we compared the levels of active Nrf2 between nuclear extracts of treated and untreated H9c2 cells, and between nuclear extracts from control and treated mouse hearts. We found a six-fold increase in Nrf2 activity in SFN-treated H9c2 cells and a fourfold increase in SFN+DOX-treated cells (Fig. 11). Similarly, active Nrf2 in the nuclear extracts

from SFN-treated murine hearts was over 50% higher as compared to control mice (Fig. 11). DOX treatment alone lowered Nrf2 activity; but it remained significantly higher in the SFN +DOX versus DOX-treated hearts.

SFN treatment counters the DOX-induced down-regulation of antioxidant and anti-electrophile enzymes *in vivo*

To elucidate the mechanisms of SFN-mediated protection of cardiac tissue during DOX treatment in mice, we examined the expression of a number of genes related to oxidant and electrophile metabolism. The selected genes (Table 2) fell into three functionally distinct classes which are known to be regulated by Nrf2 [71] : antioxidant, anti-electrophile, and genes involved in glutathione synthesis. Transcript levels of a number of antioxidant and anti-electrophile genes were increased in hearts from SFN+DOX-treated mice, as compared to those treated with DOX alone (Table 2). This shift in metabolism may explain why SFN treatment of mice is cardioprotective during DOX treatment. A direct comparison of transcript levels specifically for *catalase, Sod1, Sod2, HO1, Nqo1* and *Gsta4* in hearts of treated and control mice showed that expression of these genes was significantly higher in SFN-treated animals (Table 2). *In silico* or *in vitro* analysis of the *Gsta4, Nqo-1, Ho-1* and *Sod2* promoter regions revealed consensus ARE binding sites for the Nfe2l2 (Nrf2) transcription factor [72-75]. On the other hand, most of the examined transcript levels (with the exception of *Pxdn, Gpx4, Txnrd1, Gsta1+2, Gsta3, Gstm1, Aor*and *Gclm*) were expressed at lower levels in the DOX-treated group. The resulting lower level of antioxidant and anti-electrophilic defense mechanisms in DOX-treated versus control animals, could contribute to the oxidative damage in the heart. In contrast, in SFN+DOX treated animals, levels of all the transcripts, except *Akr3*, were essentially similar to those of the control group, suggesting an SFN-mediated reversal of the effects of DOX on these gene activities. Similarly, western blot analyses of cardiac extracts prepared from mice treated with DOX, SFN and DOX+SFN indicated that while the expression of GSTA4-4, SOD2, NQO1 and HO-1 was down-regulated in hearts treated with DOX alone, a combined treatment of DOX +SFN significantly prevented this down-regulation (Fig. 12).

Discussion

DOX-induced cardiotoxicity has been shown to be mediated through several mechanisms including free radical generation, membrane lipid peroxidation (LPO), mitochondrial damage and iron-dependent oxidative damage to macromolecules [9, 17]. Several studies have demonstrated that DOX induces the generation of a cascade of reactive oxygen species (ROS) such as oxyanions, hydroxyl radicals and hydrogen peroxide, which are implicated in DOX-induced cardiomyopathy [76, 77]. Enhanced generation of electrophiles and oxidants during DOX therapy stimulates the oxidation of membrane lipids leading to the accumulation of the highly reactive electrophile, 4-HNE, which has been shown to modify protein functions, affect mitochondrial function in and be a particularly good biomarker of DOX-induced oxidative stress [32]. DOX treatment also results in depletion of glutathione (GSH) levels in the heart [78].

We recently reported that elevated Nrf2 activity in the absence of an 4-HNE-metabolizing enzyme, in *Glutathione transferase a4* null (*Gsta4*$^{-/-}$) mice, drives cellular defenses that confer protection from DOX-induced cardiomyopathy [45]. Enhanced Nrf2 signaling and cytoprotective gene activity induced by SFN have been demonstrated in cardiac cells [40, 41] *in vivo*, in primary cardiomyocytes, and extensively in the H9c2 cell line, derived from rat atrial cardiomyoblasts [40]. Our studies were designed to test the hypothesis that substantial Nrf2 activation, through SFN induction, is required for sufficient cardioprotection during DOX therapy to avoid long-term cardiomyopathy.

Before undertaking an *in vivo* study to determine if through the Keap1/Nrf2 pathway SFN could confer protection against DOX-induced cardiotoxicity, we tested our hypothesis *in vitro* by treating H9c2 cells with DOX, SFN or SFN+DOX and assaying for cell viability. Co-treatment of H9c2 cells with very low concentrations of SFN resulted in marked protection against DOX toxicity. This represents the first time that SFN was shown to increase viability of DOX-treated H9c2 cells. Furthermore, when nuclear extracts isolated from control or treated cells were assayed for Nrf2-ARE binding, SFN treatment alone not only enhanced Nrf2 binding activity in the absence of DOX, but SFN also induced Nrf2 activity very significantly in the SFN+DOX-treated group. The essential role of Nrf2 in the protective effects of SFN on DOX cardiotoxicity is further supported by the viability data obtained with the Nrf2-expressing and -depleted (Nrf2 siRNA-treated) H9c2 cells (Fig. 1) and directly indicated that SFN protected these cells in an Nrf2-dependent manner. Taken together, these results clearly suggested that SFN pretreatment of H9c2 cells protects against DOX toxicity through activation of Nrf2 and its associated upregulation of anti-oxidant and anti-electrophile enzyme expression.

Hearts of cancer patients undergoing DOX therapy are highly sensitive to DOX-induced oxidative stress. The heart expresses low levels of antioxidant enzymes, rendering it particularly vulnerable to free radical damage and DOX cardiotoxicity [11, 12]. DOX-induced cardiomyopathy, as a manifestation of chronic cardiotoxicity, presents with electrocardiographic abnormalities including ventricular dysfunction. Monitoring of left ventricle ejection fraction (EF) and fractional shortening (FS) is among the most commonly used methods for assessing early anthracycline-related cardiotoxicity. Our results from cardiac function tests and histological analysis suggest that treatment of 129/sv mice with SFN markedly protects against DOX-induced cardiomyopathy *in vivo*. Furthermore, plasma troponin levels are frequently used as a diagnostic marker for various heart disorders including DOX-induced heart muscle damage [79]. Troponin is a complex of three regulatory proteins (troponin C, troponin I, and troponin T), attached to the actin filament in skeletal or cardiac muscle tissue, and is essential to muscle contraction. While increased release of plasma cTnI in the DOX-treated mice of our study was in line with earlier studies [61, 62, 80], these levels were significantly decreased in the SFN+DOX treated mice. Our results from cardiac function tests, cTnl levels, and histopathological data suggest not only that DOX-induced cardiac failure was the primary cause of death in the mice but that cardiac failure could be reversed in large part by SFN pre- and co-treatment.

The mitochondrion is involved in stress signaling as well as energy production. Due to the high energy requirement of cardiomyocytes, mitochondria occupy ≥30-40% of cardiac cell

volume. As DOX accumulates in mitochondria, extensive oxidative and electrophilic stress initiates mitochondrial injury [81, 82]. Cardiac damage follows from highly reactive DOX metabolites, which continue a vicious cycle of oxidative/electrophilic stress [83, 84]. 4-HNE accumulating during DOX treatment modifies several mitochondrial proteins involved in energy metabolism [32]. Mitochondrial dysfunction with consequent oxidative stress, calcium and iron overload, and cardiomyocyte death as DOX side effects, leads to cardiac dysfunction [82, 85]. Expression of several key mitochondrial antioxidant enzymes, including SOD2 and catalase, is under control of Nrf2 [41, 86]. Furthermore, DOX specifically represses mitochondrial gene expression critical for mitochondrial ETC function [80]. Data obtained from our HRR study on heart biopsy samples clearly indicate that DOX therapy compromises functions of complex-I, II+III and IV. Surprisingly, the oxygen flux in SFN-only treated groups showed no significant change and is the subject of our further study. Mitochondrial complex activities in ventricular cardiomyocytes from the SFN+DOX-treated group were fully restored to the levels in the vehicle-treated control group of animals. Furthermore, the reduced level of 4-HNE-protein adducts following SFN+DOX treatment likely also contributed to improved mitochondrial function and points to a protective role for SFN, via activation of Nrf2-dependent cellular defenses.

We further examined if SFN stimulates Nrf2 activity, as a central regulator of cellular responses to oxidative and electrophilic stress, in the presence of systemic DOX. To test this, we determined the amount of active nuclear Nrf2 in the hearts of SFN and/or DOX-treated and control mice. Hearts of SFN-only treated mice showed a significant increase in ARE-binding activity while DOX treatment alone significantly reduced this activity. The drop in Nrf2 activity in the DOX-treated group of mice clearly indicated an inability of the heart, which already expresses low levels of protective enzymes, to protect itself against long-term DOX-induced oxidative and electrophilic assault. In contrast, following SFN and DOX co-treatment, Nrf2 binding activity remained significantly higher than it was during DOX treatment alone. Since SFN pre- and co-treatment significantly protect Nrf2 activity during the four-week DOX treatment in our study, overall cardioprotection would appear to operate in large part via the Nrf2 pathway.

To further establish the role of Nrf2 in our model of enhanced protection against DOX toxicity, we analyzed transcript levels of genes responsible for expression of antioxidant, anti-electrophile and glutathione synthesis pathway enzymes in the hearts of control and treated mice. DOX treatment repressed transcript levels of genes encoding antioxidant enzymes responsible for metabolism of O^{2-} and anti-electrophile enzymes responsible for removal of 4-HNE and lipid aldehydes, in the mouse heart. On the other hand, transcript levels of gene encoding anti-oxidants and anti-electrophiles were high in the SFN-treated group. However, combined SFN and DOX treatment maintained the transcript levels at control levels. These findings are consistent with our finding of the loss in Nrf2-ARE binding activity during DOX treatment and increase in Nrf2 activity in SFN+DOX treated mice. Repression of some critical gene expression by DOX and then recovery of normal protein levels by combined SFN+DOX treatment was confirmed by western blot analysis for the *Gsta4*, *Sod2*, *Nqo1* and *Ho-1* gene products. Quantitative PCR and complimentary western blot data clearly suggest that under our experimental conditions, DOX represses

expression of specific antioxidant and anti-electrophile enzymes. On the other hand, SFN treatment maintains or even upregulates enzymes involved in scavenging or neutralizing of free radicals, in oxygen quenching and making it and lipid peroxidation products less available for oxidative/electrophilic stress. Our finding clearly suggests that transcriptional activation, by Nrf2, of genes expressing anitoxidants and anti-electrophile enzymes can play a critical role during DOX therapy. Thus, SFN could effectively prevent heart tissue damage during DOX therapy not only by decreasing the oxidative/electrophilic stress, but by restoring multiple cardiac cellular defenses through other activities of the Keap1/Nrf2 pathway, such as autophagy [87].

GSH acts as an antioxidant and inhibits lipid peroxidation during stress. GSH also participates in the detoxification of hydrogen peroxide by various glutathione peroxidases and is the substrate for GSTs to conjugate the lipid peroxidation product, 4-HNE. It is well documented that SFN treatment induces the expression of the requisite genes for GSH synthesis in cultured cells and in rodents [88-90]. In particular, SFN exerts its inducing effect on glutamate cysteine ligase via Nrf2 signaling [90]. The levels for glutamate cysteine ligase catalytic (*Gclc*) and modifier (*Gclm*) subunit mRNAs, the latter catalyzing the rate-limiting step of glutathione synthesis, were examined in cardiac tissues of our DOX, SFN and SFN+DOX-treated mice. While these analyses showed an increase in *Gclc* mRNA in the SFN-treated group, *Gclc* mRNA levels, like other Nrf2-regulated transcripts under our experimental conditions, were significantly lower than control in the DOX-treated group. However, in the SFN+DOX-treated group, SFN was able to block the DOX-mediated repression of the *Gcl* catalytic unit.

In summary, DOX is a very valuable cancer chemotherapeutic drug that frequently results in severe cardiomyopathy. The ability of SFN to protect against DOX cardiotoxicity, as shown for the first time by the results of our study, is a discovery that could significantly change the way DOX is currently used. Our findings not only provide further insight into DOX-induced cardiotoxicity, but especially demonstrate SFN action through the Keap1/Nrf2 signaling pathway for countering cardiac damage. Our observations should establish the basis for devising novel approaches to protect the human heart from the harmful effects of cardiotoxic drugs, which are thought to be mediated in part by oxidative stress signaling.

Supplementary Material

Refer to Web version on PubMed Central for supplementary material.

Acknowledgements

This work was supported in part by a grant from the National Institutes of Health (R01 AG032643 to Sharda P. Singh) and a grant from the American Heart Association (14GRNT18890084 to Sharda P. Singh). The authors would like to thank Dr. Lee Ann MacMillan-Crow for her advice and experimental protocol for the HRR study.

Abbreviations

DOX doxorubicin

SFN	sulforaphane
Nrf2	Nuclear factor erythroid 2-related factor 2
ARE	antioxidant responsive element
Keap1	kelch-like ECH-associated protein-1
Cul3	cullin 3
GCLC	catalytic subunit of glutamate-cysteine ligase
GCLM	modify subunit of glutamate-cysteine ligase
HO-1	heme oxygenase 1
NQO1	NAD(P)H dehydrogenase,quinone 1
GSTA4-4	glutathione S-transferase alpha 4
SOD2	superoxide dismutase 2
ROS	reactive oxygen species
AMC	amino-4-methyl coumarin
DEVD	Asp-Glu-Val-Asp
HRR	high resolution respirometry

References

[1]. Joshi G, Sultana R, Tangpong J, Cole MP, St Clair DK, Vore M, Estus S, Butterfield DA. Free radical mediated oxidative stress and toxic side effects in brain induced by the anti cancer drug adriamycin: insight into chemobrain. Free Radic. Res. 2005; 39:1147–1154. [PubMed: 16298740]

[2]. Prados J, Melguizo C, Ortiz R, Velez C, Alvarez PJ, Arias JL, Ruiz MA, Gallardo V, Aranega A. Doxorubicin-loaded nanoparticles: new advances in breast cancer therapy. Anticancer Agents Med. Chem. 2012; 12:1058–1070. [PubMed: 22339066]

[3]. Chaiswing L, Cole MP, St Clair DK, Ittarat W, Szweda LI, Oberley TD. Oxidative damage precedes nitrative damage in adriamycin-induced cardiac mitochondrial injury. Toxicol. Pathol. 2004; 32:536–547. [PubMed: 15605432]

[4]. Thorn CF, Oshiro C, Marsh S, Hernandez-Boussard T, McLeod H, Klein TE, Altman RB. Doxorubicin pathways: pharmacodynamics and adverse effects. Pharmacogenet. Genomics. 2011; 21:440–446. [PubMed: 21048526]

[5]. Harake D, Franco VI, Henkel JM, Miller TL, Lipshultz SE. Cardiotoxicity in childhood cancer survivors: strategies for prevention and management. Future Cardiol. 2012; 8:647–670. [PubMed: 22871201]

[6]. Jensen BC, McLeod HL. Pharmacogenomics as a risk mitigation strategy for chemotherapeutic cardiotoxicity. Pharmacogenomics. 2013; 14:205–213. [PubMed: 23327580]

[7]. Menna P, Gonzalez Paz O, Chello M, Covino E, Salvatorelli E, Minotti G. Anthracycline cardiotoxicity. Expert Opinion on Drug Safety. 2012; 11:S21–S36. [PubMed: 21635149]

[8]. Rahman AM, Yusuf SW, Ewer MS. Anthracycline-induced cardiotoxicity and the cardiac-sparing effect of liposomal formulation. Int J Nanomedicine. 2007; 2:567–583. [PubMed: 18203425]

[9]. Carvalho FS, Burgeiro A, Garcia R, Moreno AJ, Carvalho RA, Oliveira PJ. Doxorubicin-induced cardiotoxicity: from bioenergetic failure and cell death to cardiomyopathy. Med. Res. Rev. 2014; 34:106–135. [PubMed: 23494977]

[10]. Sterba M, Popelova O, Vavrova A, Jirkovsky E, Kovarikova P, Gersl V, Simunek T. Oxidative stress, redox signaling, and metal chelation in anthracycline cardiotoxicity and pharmacological cardioprotection. Antioxid Redox Signal. 2013; 18:899–929. [PubMed: 22794198]

[11]. Maksimenko AV, Vavaev AV. Antioxidant enzymes as potential targets in cardioprotection and treatment of cardiovascular diseases. Enzyme antioxidants: the next stage of pharmacological counterwork to the oxidative stress. Heart Int. 2012; 7:e3. [PubMed: 22690296]

[12]. Todorova VK, Beggs ML, Delongchamp RR, Dhakal I, Makhoul I, Wei JY, Klimberg VS. Transcriptome profiling of peripheral blood cells identifies potential biomarkers for Doxorubicin cardiotoxicity in a rat model. PLoS One. 2012; 7:e48398. [PubMed: 23209553]

[13]. Minotti G, Menna P, Salvatorelli E, Cairo G, Gianni L. Anthracyclines: molecular advances and pharmacologic developments in antitumor activity and cardiotoxicity. Pharmacol. Rev. 2004; 56:185–229. [PubMed: 15169927]

[14]. Kresh JY, Chopra A. Intercellular and extracellular mechanotransduction in cardiac myocytes. Pflugers Arch. 2011; 462:75–87. [PubMed: 21437600]

[15]. Dolinsky VW, Dyck JR. Calorie restriction and resveratrol in cardiovascular health and disease. Biochim. Biophys. Acta. 2011; 1812:1477–1489. [PubMed: 21749920]

[16]. Xi L, Zhu SG, Das A, Chen Q, Durrant D, Hobbs DC, Lesnefsky EJ, Kukreja RC. Dietary inorganic nitrate alleviates doxorubicin cardiotoxicity: mechanisms and implications. Nitric Oxide. 2012; 26:274–284. [PubMed: 22484629]

[17]. Pereira GC, Silva AM, Diogo CV, Carvalho FS, Monteiro P, Oliveira PJ. Drug-induced cardiac mitochondrial toxicity and protection: from doxorubicin to carvedilol. Curr. Pharm. Des. 2011; 17:2113–2129. [PubMed: 21718248]

[18]. Deavall DG, Martin EA, Horner JM, Roberts R. Drug-induced oxidative stress and toxicity. J. Toxicol. 2012; 2012:645460. [PubMed: 22919381]

[19]. Forman HJ, Davies KJA, Ursini F. How do nutritional antioxidants really work: Nucleophilic tone and para-hormesis versus free radical scavenging in vivo. Free Radic. Biol. Med. 2014; 66:24–35. [PubMed: 23747930]

[20]. Kaspar JW, Niture SK, Jaiswal AK. Nrf2:INrf2 (Keap1) signaling in oxidative stress. Free Radic. Biol. Med. 2009; 47:1304–1309. [PubMed: 19666107]

[21]. Niture SK, Khatri R, Jaiswal AK. Regulation of Nrf2-an update. Free Radic. Biol. Med. 2014; 66:36–44. [PubMed: 23434765]

[22]. Ma Q. Role of Nrf2 in Oxidative Stress and Toxicity. Annu. Rev. Pharmacol. Toxicol. 2013; 53:401–426. [PubMed: 23294312]

[23]. Muthusamy VR, Kannan S, Sadhaasivam K, Gounder SS, Davidson CJ, Boeheme C, Hoidal JR, Wang L, Rajasekaran NS. Acute exercise stress activates Nrf2/ARE signaling and promotes antioxidant mechanisms in the myocardium. Free Radic. Biol. Med. 2012; 52:366–376. [PubMed: 22051043]

[24]. Brewer AC, Murray TV, Arno M, Zhang M, Anilkumar NP, Mann GE, Shah AM. Nox4 regulates Nrf2 and glutathione redox in cardiomyocytes in vivo. Free Radic. Biol. Med. 2011; 51:205–215. [PubMed: 21554947]

[25]. Anfossi G, Russo I, Trovati M. Platelet dysfunction in central obesity. Nutrition Metabolism and Cardiovascular Diseases. 2009; 19:440–449.

[26]. Mann GE, Niehueser-Saran J, Watson A, Gao L, Ishii T, de Winter P, Siow RC. Nrf2/ARE regulated antioxidant gene expression in endothelial and smooth muscle cells in oxidative stress: implications for atherosclerosis and preeclampsia. Sheng lixue bao : [Acta physiologica Sinica]. 2007; 59:117–127.

[27]. Cao Z, Zhu H, Zhang L, Zhao X, Zweier JL, Li Y. Antioxidants and phase 2 enzymes in cardiomyocytes: Chemical inducibility and chemoprotection against oxidant and simulated ischemia-reperfusion injury. Exp. Biol. Med. (Maywood). 2006; 231:1353–1364. [PubMed: 16946404]

[28]. Kobayashi M, Li L, Iwamoto N, Nakajima-Takagi Y, Kaneko H, Nakayama Y, Eguchi M, Wada Y, Kumagai Y, Yamamoto M. The antioxidant defense system Keap1-Nrf2 comprises a multiple sensing mechanism for responding to a wide range of chemical compounds. Mol. Cell. Biol. 2009; 29:493–502. [PubMed: 19001094]

[29]. Bakdash N, Williams MS. Spatially distinct production of reactive oxygen species regulates platelet activation. Free Radic. Biol. Med. 2008; 45:158–166. [PubMed: 18452718]

[30]. Aldini G, Dalle-Donne I, Colombo R, Maffei Facino R, Milzani A, Carini M. Lipoxidation-derived reactive carbonyl species as potential drug targets in preventing protein carbonylation and related cellular dysfunction. ChemMedChem. 2006; 1:1045–1058. [PubMed: 16915603]

[31]. Kansanen E, Bonacci G, Schopfer FJ, Kuosmanen SM, Tong KI, Leinonen H, Woodcock SR, Yamamoto M, Carlberg C, Yla-Herttuala S, Freeman BA, Levonen AL. Electrophilic nitro-fatty acids activate NRF2 by a KEAP1 cysteine 151-independent mechanism. J. Biol. Chem. 2011; 286:14019–14027. [PubMed: 21357422]

[32]. Zhao Y, Miriyala S, Miao L, Mitov M, Schnell D, Dhar SK, Cai J, Klein JB, Sultana R, Butterfield DA, Vore M, Batinic-Haberle I, Bondada S, St Clair DK. Redox proteomic identification of HNE-bound mitochondrial proteins in cardiac tissues reveals a systemic effect on energy metabolism after doxorubicin treatment. Free Radic. Biol. Med. 2014; 72:55–65. [PubMed: 24632380]

[33]. Veeranki OL, Bhattacharya A, Marshall JR, Zhang Y. Organ-specific exposure and response to sulforaphane, a key chemopreventive ingredient in broccoli: implications for cancer prevention. Br. J. Nutr. 2013; 109:25–32. [PubMed: 22464629]

[34]. Kensler, T.; Egner, P.; Agyeman, A.; Visvanathan, K.; Groopman, J.; Chen, J-G.; Chen, T-Y.; Fahey, J.; Talalay, P. Keap1-Nrf2 Signaling: A Target for Cancer Prevention by Sulforaphane. In: Pezzuto, JM.; Suh, N., editors. Natural Products in Cancer Prevention and Therapy. Springer; Berlin Heidelberg: 2013. p. 163-177.

[35]. Singh SV, Warin R, Xiao D, Powolny AA, Stan SD, Arlotti JA, Zeng Y, Hahm ER, Marynowski SW, Bommareddy A, Desai D, Amin S, Parise RA, Beumer JH, Chambers WH. Sulforaphane inhibits prostate carcinogenesis and pulmonary metastasis in TRAMP mice in association with increased cytotoxicity of natural killer cells. Cancer Res. 2009; 69:2117–2125. [PubMed: 19223537]

[36]. Biswas S, Hwang JW, Kirkham PA, Rahman I. Pharmacological and dietary antioxidant therapies for chronic obstructive pulmonary disease. Curr. Med. Chem. 2013; 20:1496–1530. [PubMed: 22963552]

[37]. Ahn YH, Hwang Y, Liu H, Wang XJ, Zhang Y, Stephenson KK, Boronina TN, Cole RN, Dinkova-Kostova AT, Talalay P, Cole PA. Electrophilic tuning of the chemoprotective natural product sulforaphane. Proc. Natl. Acad. Sci. U. S. A. 2010; 107:9590–9595. [PubMed: 20439747]

[38]. Hu C, Eggler AL, Mesecar AD, van Breemen RB. Modification of keap1 cysteine residues by sulforaphane. Chem. Res. Toxicol. 2011; 24:515–521. [PubMed: 21391649]

[39]. Zhang DD. Mechanistic studies of the Nrf2-Keap1 signaling pathway. Drug Metab. Rev. 2006; 38:769–789. [PubMed: 17145701]

[40]. Bai Y, Cui W, Xin Y, Miao X, Barati MT, Zhang C, Chen Q, Tan Y, Cui T, Zheng Y, Cai L. Prevention by sulforaphane of diabetic cardiomyopathy is associated with up-regulation of Nrf2 expression and transcription activation. J. Mol. Cell. Cardiol. 2013; 57C:82–95. [PubMed: 23353773]

[41]. Piao CS, Gao S, Lee GH, Kim do S, Park BH, Chae SW, Chae HJ, Kim SH. Sulforaphane protects ischemic injury of hearts through antioxidant pathway and mitochondrial K(ATP) channels. Pharmacol. Res. 2010; 61:342–348. [PubMed: 19948220]

[42]. Angeloni C, Leoncini E, Malaguti M, Angelini S, Hrelia P, Hrelia S. Modulation of phase II enzymes by sulforaphane: implications for its cardioprotective potential. Journal of Agricultural and Food Chemis ry. 2009; 57:5615–5622.

[43]. McElhanon KE, Bose C, Sharma R, Wu L, Awasthi YC, Singh SP. Gsta4 Null Mouse Embryonic Fibroblasts Exhibit Enhanced Sensitivity to Oxidants: Role of 4-Hydroxynonenal in Oxidant Toxicity. Open Journal of Apoptosis. 2013; 2:11.

[44]. Kaushal GP, Kaushal V, Hong X, Shah SV. Role and regulation of activation of caspases in cisplatin-induced injury to renal tubular epithelial cells. Kidney Int. 2001; 60:1726–1736. [PubMed: 11703590]

[45]. Benes H, Vuong MK, Boerma M, McElhanon KE, Siegel ER, Singh SP. Protection from Oxidative and Electrophilic Stress in the Gsta4-null Mouse Heart. Cardiovasc. Toxicol. 2013; 13:347–356. [PubMed: 23690225]

[46]. Zimniak P. Relationship of electrophilic stress to aging. Free Radic. Biol. Med. 2011; 51:1087–1105. [PubMed: 21708248]

[47]. Satoh K, Yamada S, Koike Y, Igarashi Y, Toyokuni S, Kumano T, Takahata T, Hayakari M, Tsuchida S, Uchida K. A 1-Hour Enzyme-Linked Immunosorbent Assay for Quantitation of Acrolein- and Hydroxynonenal-Modified Proteins by Epitope-Bound Casein Matrix Method. Anal. Biochem. 1999; 270:323–328. [PubMed: 10334850]

[48]. Ayyadevara S, Dandapat A, Singh SP, Siegel ER, Shmookler Reis RJ, Zimniak L, Zimniak P. Life span and stress resistance of Caenorhabditis elegans are differentially affected by glutathione transferases metabolizing 4-hydroxynon-2-enal. Mech. Ageing Dev. 2007; 128:196–205. [PubMed: 17157356]

[49]. Kuznetsov AV, Schneeberger S, Seiler R, Brandacher G, Mark W, Steurer W, Saks V, Usson Y, Margreiter R, Gnaiger E. Mitochondrial defects and heterogeneous cytochrome c release after cardiac cold ischemia and reperfusion. Am. J. Physiol. Heart Circ. Physiol. 2004; 286:H1633–1641. [PubMed: 14693685]

[50]. Hughey CC, Hittel DS, Johnsen VL, Shearer J. Respirometric oxidative phosphorylation assessment in saponin-permeabilized cardiac fibers. J Vis Exp. 2011

[51]. Parajuli N, Campbell LH, Marine A, Brockbank KG, Macmillan-Crow LA. MitoQ blunts mitochondrial and renal damage during cold preservation of porcine kidneys. PLoS One. 2012; 7:e48590. [PubMed: 23139796]

[52]. Singh SP, Niemczyk M, Saini D, Sadovov V, Zimniak L, Zimniak P. Disruption of the mGsta4 gene increases life span of C57BL mice. Journals of Gerontology. Series A, Biological Sciences and Medical Sciences. 2010; 65:14–23.

[53]. Singh SP, Niemczyk M, Saini D, Awasthi YC, Zimniak L, Zimniak P. Role of the electrophilic lipid peroxidation product 4-hydroxynonenal in the development and maintenance of obesity in mice. Biochemistry. 2008; 47:3900–3911. [PubMed: 18311940]

[54]. Singh SP, Janecki AJ, Srivastava SK, Awasthi S, Awasthi YC, Xia SJ, Zimniak P. Membrane association of glutathione S-transferase mGSTA4-4, an enzyme that metabolizes lipid peroxidation products. J. Biol. Chem. 2002; 277:4232–4239. [PubMed: 11714719]

[55]. Mukherjee S, Gangopadhyay H, Das DK. Broccoli: a unique vegetable that protects mammalian hearts through the redox cycling of the thioredoxin superfamily. Journal of Agricultural and Food Chemistry. 2008; 56:609–617. [PubMed: 18163565]

[56]. Zhu H, Zhang L, Xi X, Zweier JL, Li Y. 4-Hydroxy-2-nonenal upregulates endogenous antioxidants and phase 2 enzymes in rat H9c2 myocardiac cells: protection against overt oxidative and electrophilic injury. Free Radic. Res. 2006; 40:875–884. [PubMed: 17015266]

[57]. Zhang Y, Sano M, Shinmura K, Tamaki K, Katsumata Y, Matsuhashi T, Morizane S, Ito H, Hishiki T, Endo J, Zhou H, Yuasa S, Kaneda R, Suematsu M, Fukuda K. 4-hydroxy-2-nonenal protects against cardiac ischemia-reperfusion injury via the Nrf2-dependent pathway. J. Mol. Cell. Cardiol. 2010; 49:576–586. [PubMed: 20685357]

[58]. Sawyer DB, Fukazawa R, Arstall MA, Kelly RA. Daunorubicin-induced apoptosis in rat cardiac myocytes is inhibited by dexrazoxane. Circ. Res. 1999; 84:257–265. [PubMed: 10024299]

[59]. Tan X, Wang DB, Lu X, Wei H, Zhu R, Zhu SS, Jiang H, Yang ZJ. Doxorubicin induces apoptosis in H9c2 cardiomyocytes: role of overexpressed eukaryotic translation initiation factor 5A. Biol. Pharm. Bull. 2010; 33:1666–1672. [PubMed: 20930373]

[60]. Spagnuolo RD, Recalcati S, Tacchini L, Cairo G. Role of hypoxia-inducible factors in the dexrazoxane-mediated protection of cardiomyocytes from doxorubicin-induced toxicity. Br. J. Pharmacol. 2011; 163:299–312. [PubMed: 21232037]

[61]. Desai VG, Herman EH, Moland CL, Branham WS, Lewis SM, Davis KJ, George NI, Lee T, Kerr S, Fuscoe JC. Development of doxorubicin-induced chronic cardiotoxicity in the B6C3F1 mouse model. Toxicol. Appl. Pharmacol. 2013; 266:109–121. [PubMed: 23142469]

[62]. Lipshultz SE, Miller TL, Scully RE, Lipsitz SR, Rifai N, Silverman LB, Colan SD, Neuberg DS, Dahlberg SE, Henkel JM, Asselin BL, Athale UH, Clavell LA, Laverdiere C, Michon B, Schorin

MA, Sallan SE. Changes in Cardiac Biomarkers During Doxorubicin Treatment of Pediatric Patients With High-Risk Acute Lymphoblastic Leukemia: Associations With Long-Term Echocardiographic Outcomes. J. Clin. Oncol. 2012

[63]. Todorova VK, Kaufmann Y, Klimberg VS. Increased efficacy and reduced cardiotoxicity of metronomic treatment with cyclophosphamide in rat breast cancer. Anticancer Res. 2011; 31:215–220. [PubMed: 21273601]

[64]. Jirkovsky E, Popelova O, Krivakova-Stankova P, Vavrova A, Hroch M, Haskova P, Brcakova-Dolezelova E, Micuda S, Adamcova M, Simunek T, Cervinkova Z, Gersl V, Sterba M. Chronic anthracycline cardiotoxicity: molecular and functional analysis with focus on nuclear factor erythroid 2-related factor 2 and mitochondrial biogenesis pathways. J. Pharmacol. Exp. Ther. 2012; 343:468–478. [PubMed: 22915767]

[65]. Jungsuwadee P, Nithipongvanitch R, Chen Y, Oberley TD, Butterfield DA, St Clair DK, Vore M. Mrp1 localization and function in cardiac mitochondria after doxorubicin. Mol. Pharmacol. 2009; 75:1117–1126. [PubMed: 19233900]

[66]. Jungsuwadee P, Cole MP, Sultana R, Joshi G, Tangpong J, Butterfield DA, St Clair DK, Vore M. Increase in Mrp1 expression and 4-hydroxy-2-nonenal adduction in heart tissue of Adriamycin-treated C57BL/6 mice. Mol. Cancer Ther. 2006; 5:2851–2860. [PubMed: 17121932]

[67]. Carvalho FS, Burgeiro A, Garcia R, Moreno AJ, Carvalho RA, Oliveira PJ. Doxorubicin-Induced Cardiotoxicity: From Bioenergetic Failure and Cell Death to Cardiomyopathy. Med. Res. Rev. 2013 In Press.

[68]. Man C, Li X, Zhao D. Cloning, sequence identification, and tissue expression analysis of novel chicken NYGGF4 gene. Mol. Cell. Biochem. 2011; 346:117–124. [PubMed: 20882399]

[69]. Abarikwu SO, Pant AB, Farombi EO. 4-Hydroxynonenal induces mitochondrial-mediated apoptosis and oxidative stress in SH-SY5Y human neuronal cells. Basic Clin. Pharmacol. Toxicol. 2012; 110:441–448. [PubMed: 22118713]

[70]. Chen CH, Budas GR, Churchill EN, Disatnik MH, Hurley TD, Mochly-Rosen D. Activation of aldehyde dehydrogenase-2 reduces ischemic damage to the heart. Science. 2008; 321:1493–1495. [PubMed: 18787169]

[71]. Hayes JD, Dinkova-Kostova AT. The Nrf2 regulatory network provides an interface between redox and intermediary metabolism. Trends Biochem. Sci. 2014; 39:199–218. [PubMed: 24647116]

[72]. Cherry AD, Suliman HB, Bartz RR, Piantadosi CA. Peroxisome proliferator-activated receptor gamma co-activator 1-alpha as a critical co-activator of the murine hepatic oxidative stress response and mitochondrial biogenesis in Staphylococcus aureus sepsis. J. Biol. Chem. 2014; 289:41–52. [PubMed: 24253037]

[73]. Malhotra D, Portales-Casamar E, Singh A, Srivastava S, Arenillas D, Happel C, Shyr C, Wakabayashi N, Kensler TW, Wasserman WW, Biswal S. Global mapping of binding sites for Nrf2 identifies novel targets in cell survival response through ChIP-Seq profiling and network analysis. Nucleic Acids Res. 2010; 38:5718–5734. [PubMed: 20460467]

[74]. Ma Q, He X. Molecular Basis of Electrophilic and Oxidative Defense: Promises and Perils of Nrf2. Pharmacol. Rev. 2012; 64:1055–1081. [PubMed: 22966037]

[75]. Reichard JF, Motz GT, Puga A. Heme oxygenase-1 induction by NRF2 requires inactivation of the transcriptional repressor BACH1. Nucleic Acids Res. 2007; 35:7074–7086. [PubMed: 17942419]

[76]. Bhardwaj A, Singh S, Srivastava SK, Honkanen RE, Reed E, Singh AP. Modulation of Protein Phosphatase 2A Activity Alters Androgen-Independent Growth of Prostate Cancer Cells: Therapeutic Implications. Mol. Cancer Ther. 2011; 10:720–731. [PubMed: 21393425]

[77]. Teraoka K, Hirano M, Yamaguchi K, Yamashina A. Progressive cardiac dysfunction in adriamycin-induced cardiomyopathy rats. Eur. J. Heart Fail. 2000; 2:373–378. [PubMed: 11113713]

[78]. Al-Harthi SE, Alarabi OM, Ramadan WS, Alaama MN, Al-Kreathy HM, Damanhouri ZA, Khan LM, Osman AM. Amelioration of doxorubicininduced cardiotoxicity by resveratrol. Mol Med Rep. 2014; 10:1455–1460. [PubMed: 25059399]

[79]. Mahajan VS, Jarolim P. How to interpret elevated cardiac troponin levels. Circulation. 2011; 124:2350–2354. [PubMed: 22105197]

[80]. Thompson K, Rosenzweig B, Zhang J, Knapton A, Honchel R, Lipshultz S, Retief J, Sistare F, Herman E. Early alterations in heart gene expression profiles associated with doxorubicin cardiotoxicity in rats. Cancer Chemother. Pharmacol. 2010; 66:303–314. [PubMed: 19915844]

[81]. Kuznetsov AV, Margreiter R, Amberger A, Saks V, Grimm M. Changes in mitochondrial redox state, membrane potential and calcium precede mitochondrial dysfunction in doxorubicin-induced cell death. Biochimica et Biophysica Acta (BBA) - Molecular Cell Research. 2011; 1813:1144–1152. [PubMed: 21406203]

[82]. Ascensão A, Lumini-Oliveira J, Machado NG, Ferreira RM, Gonçalves IO, Moreira AC, Marques F, Sardao VA, Oliveira PJ, Magalhães J. Acute exercise protects against calcium-induced cardiac mitochondrial permeability transition pore opening in doxorubicin-treated rats. Clin. Sci. 2010; 120:37–49. [PubMed: 20666733]

[83]. Piquereau J, Caffin F, Novotova M, Lemaire C, Veksler V, Garnier A, Ventura-Clapier R, Joubert F. Mitochondrial dynamics in the adult cardiomyocytes: which roles for a highly specialized cell? Front. Physiol. 2013; 4:102. [PubMed: 23675354]

[84]. Montaigne D, Marechal X, Baccouch R, Modine T, Preau S, Zannis K, Marchetti P, Lancel S, Neviere R. Stabilization of mitochondrial membrane potential prevents doxorubicin-induced cardiotoxicity in isolated rat heart. Toxicol. Appl. Pharmacol. 2010; 244:300–307. [PubMed: 20096298]

[85]. Dolinsky VW, Rogan KJ, Sung MM, Zordoky BN, Haykowsky MJ, Young ME, Jones LW, Dyck JR. Both aerobic exercise and resveratrol supplementation attenuate doxorubicin-induced cardiac injury in mice. Am. J. Physiol. Endocrinol. Metab. 2013; 305:E243–253. [PubMed: 23695218]

[86]. Hybertson BM, Gao B, Bose SK, McCord JM. Oxidative stress in health and disease: the therapeutic potential of Nrf2 activation. Mol. Aspects Med. 2011; 32:234–246. [PubMed: 22020111]

[87]. Piantadosi CA, Carraway MS, Babiker A, Suliman HB. Heme Oxygenase-1 Regulates Cardiac Mitochondrial Biogenesis via Nrf2-Mediated Transcriptional Control of Nuclear Respiratory Factor-1. Circ. Res. 2008; 103:1232–1240. [PubMed: 18845810]

[88]. Dias IH, Chapple IL, Milward M, Grant MM, Hill E, Brown J, Griffiths HR. Sulforaphane restores cellular glutathione levels and reduces chronic periodontitis neutrophil hyperactivity in vitro. PLoS One. 2013; 8:e66407. [PubMed: 23826097]

[89]. Wu L, Noyan Ashraf MH, Facci M, Wang R, Paterson PG, Ferrie A, Juurlink BH. Dietary approach to attenuate oxidative stress, hypertension, and inflammation in the cardiovascular system. Proc. Natl. Acad. Sci. U. S. A. 2004; 101:7094–7099. [PubMed: 15103025]

[90]. Kim HJ, Barajas B, Wang M, Nel AE. Nrf2 activation by sulforaphane restores the age-related decrease of T(H)1 immunity: role of dendritic cells. J. Allergy Clin. Immunol. 2008; 121:1255–1261. e1257. [PubMed: 18325578]

Highlights

- Sulforaphane (SFN) protects H9c2 cardiomyoblast cells from doxorubicin (DOX) damage
- SFN protects H9c2 cells from doxorubicin damage in a Nrf2-dependent manner
- SFN and DOX co-treatment prevents DOX-induced loss of cardiac function in mice
- SFN improves mitochondrial function in hearts from DOX-treated mice
- Nuclear Nrf2 activity is upregulated and protective in SFN/DOX-treated mice

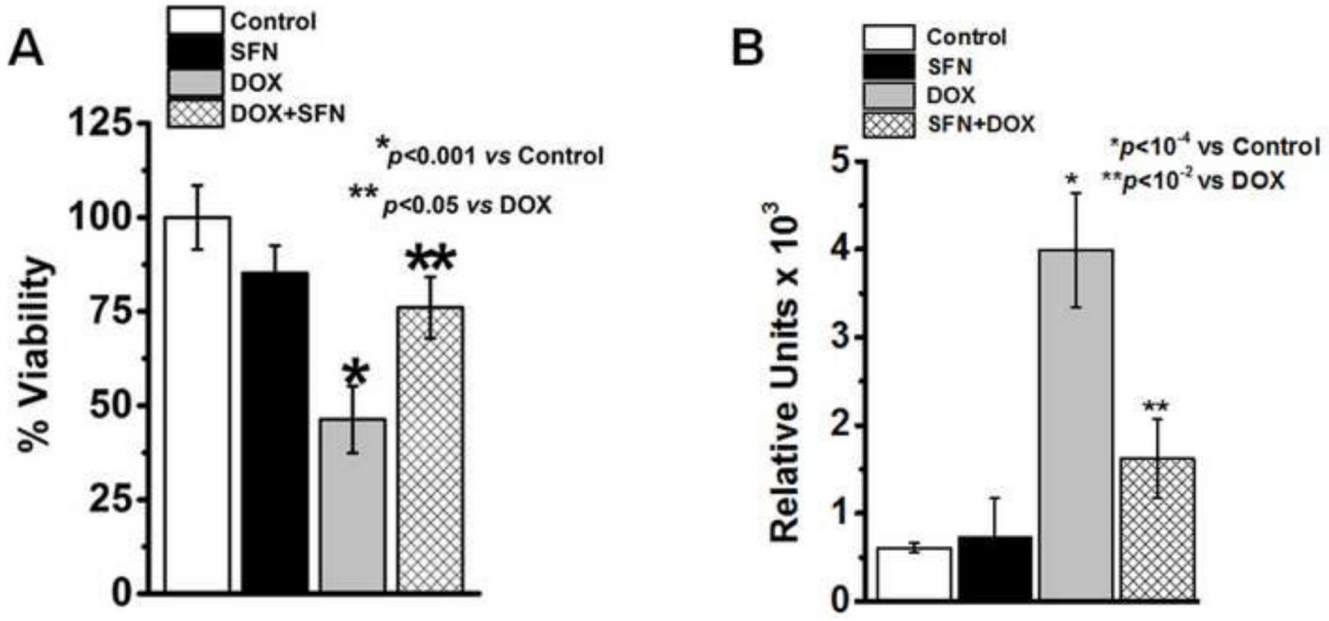

Figure 1. Quantitation of cell survival and detection of DOX-induced apoptosis in H9c2 cells

(A) H9c2 cells were treated for 24h with either 2.5 μM SFN or 5 μg/ml DOX alone, or 2.5 μM SFN + 5 μg/ml DOX. Control cells received vehicle. Cell survival was measured by the MTT assay (n=16). **(B)** H9c2 cells were treated for 24h with either 2.5 μM SFN or 5 μg/ml DOX alone, or 2.5 μM SFN + 5 μg/ml DOX. Control cells received vehicle. Caspase-3 activity was assayed using a fluorometric method (n=6).

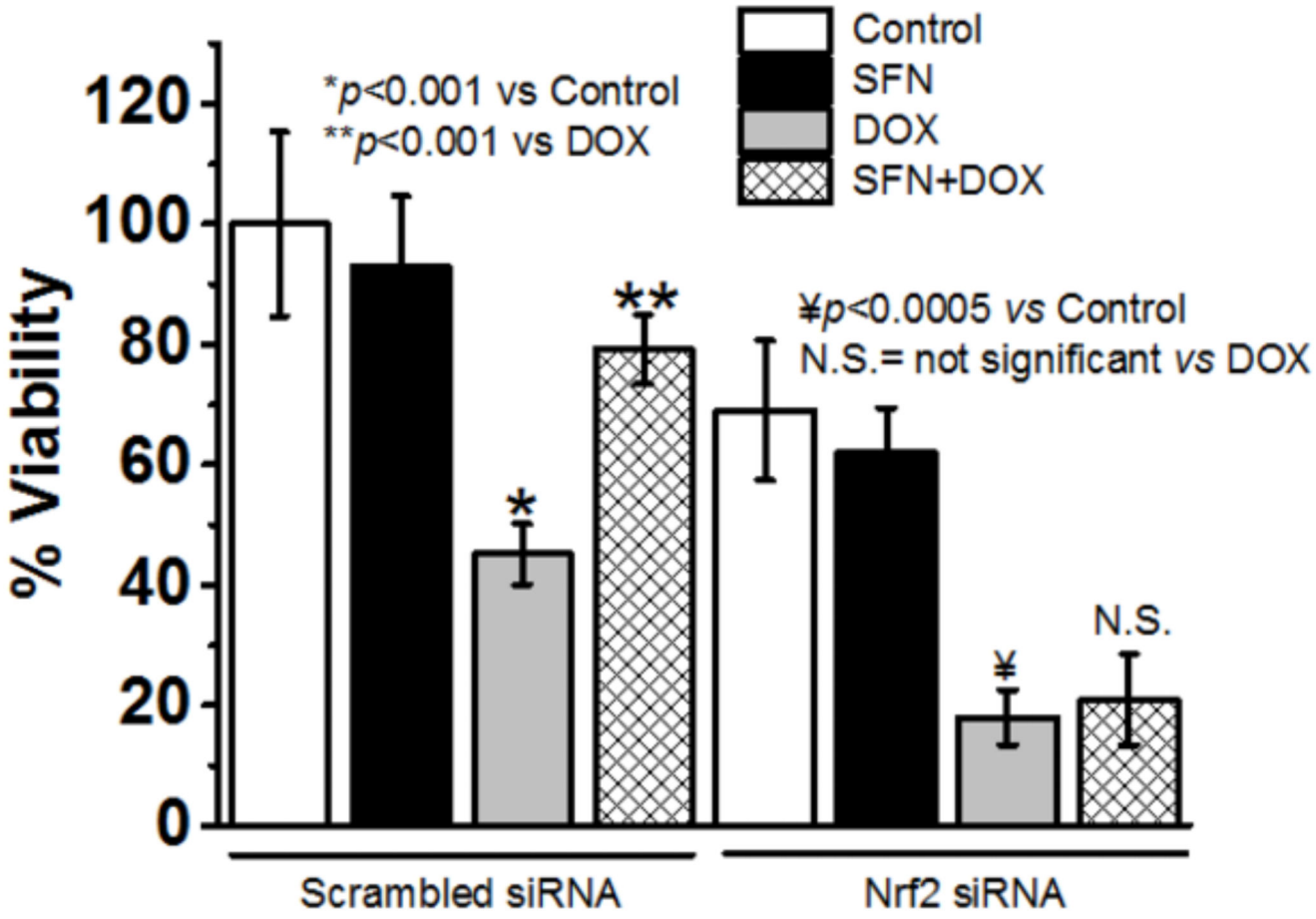

Figure 2. SFN protects cardiomyocytes from DOX toxicity in a Nrf2-dependent manner

H9c2 cells were subjected to scrambled siRNA or to *Nrf2* siRNA for 48h followed by 2.5 μM SFN and/or 5 μg/ml DOX for 24h. Viability was then determined by an LDH release assay (n=16).

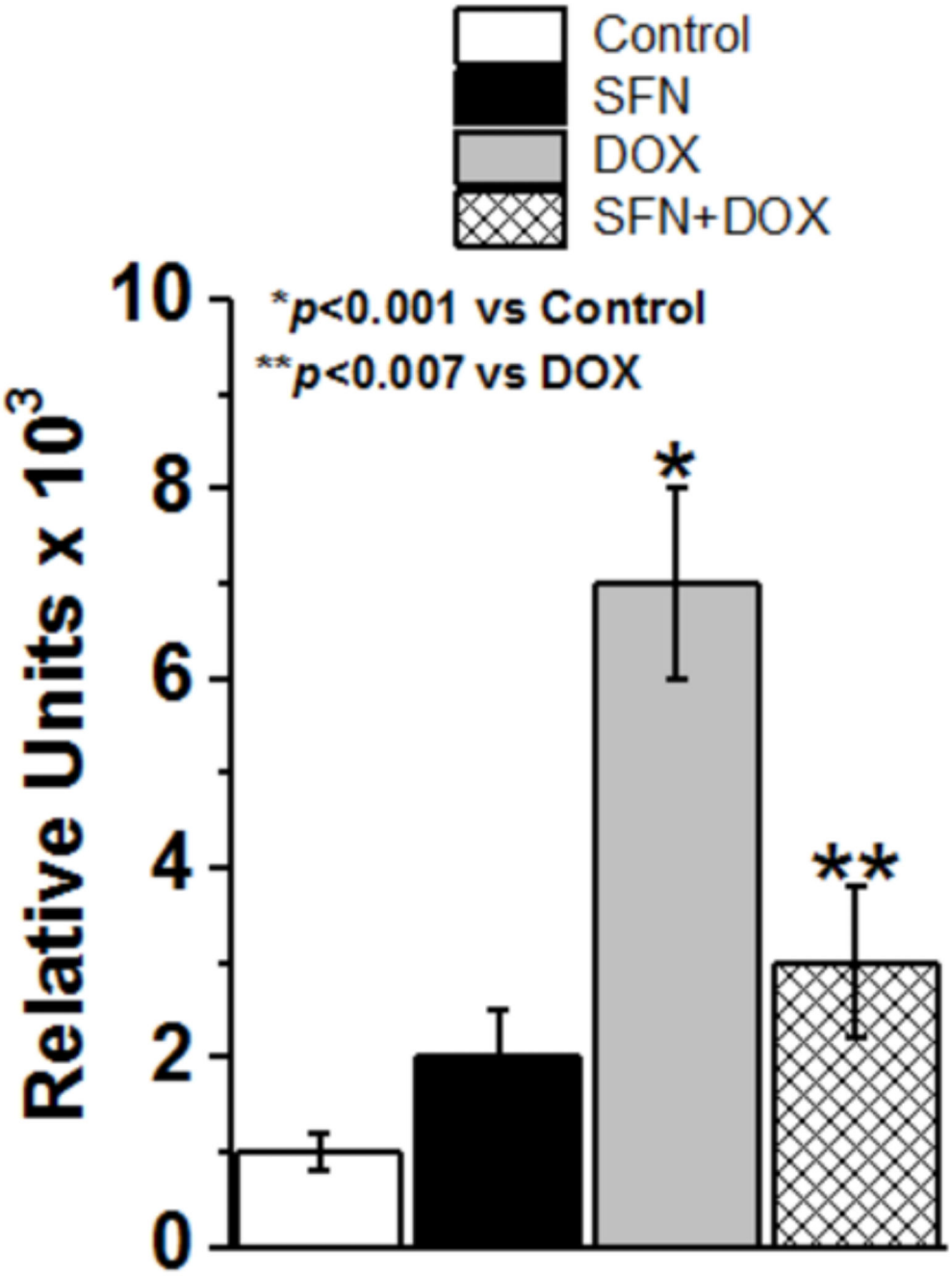

Figure 3. ROS levels in H9c2 cells treated with SFN±DOX

H9c2 cells were treated for 24h with either 2.5 μM SFN or 5 μg/ml DOX alone, or 2.5 μM SFN + 5μg/ml DOX. Control cells received vehicle. ROS production was measured using a fluorometric intracellular ROS assay kit (n=16).

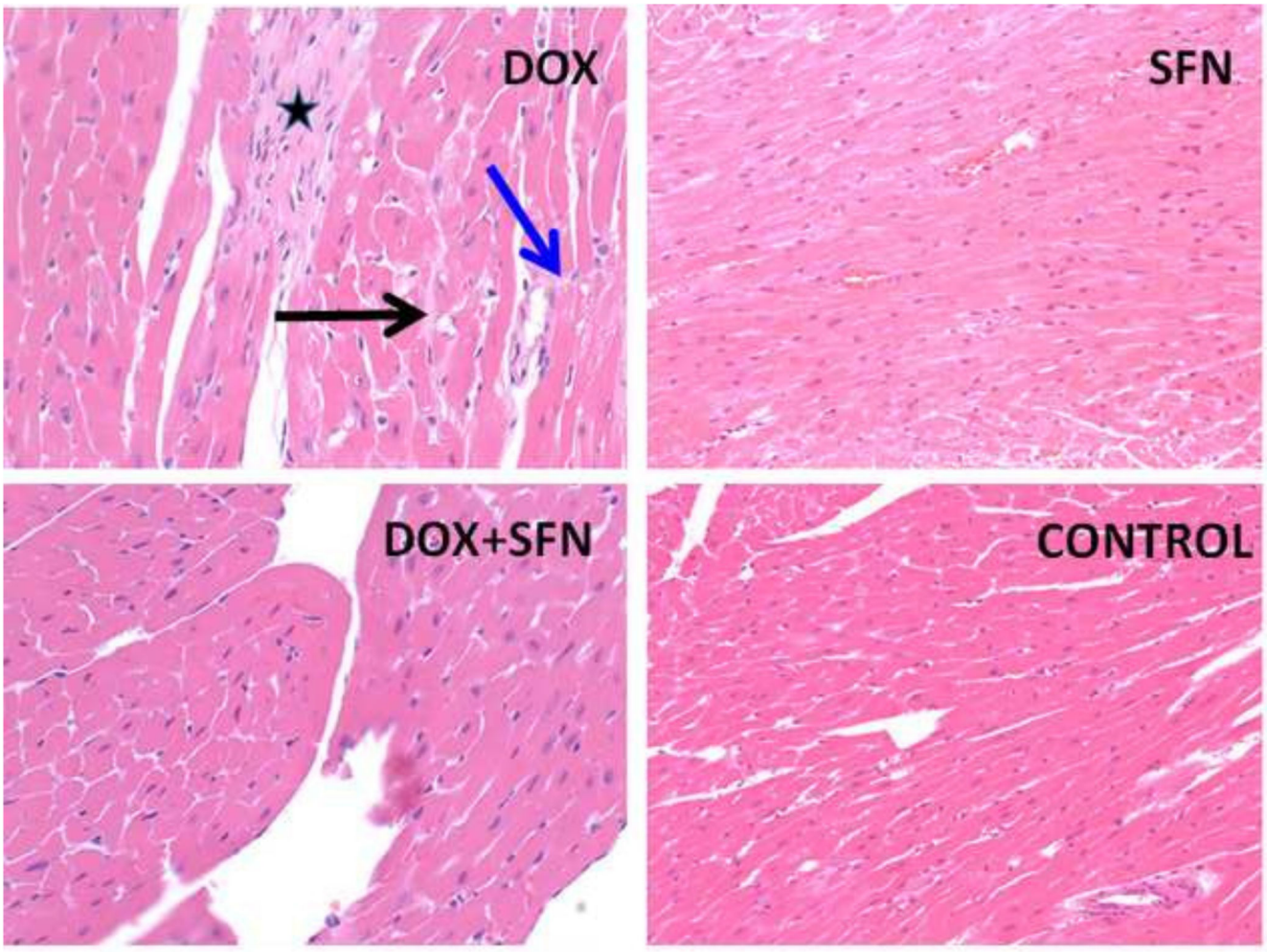

Figure 4. SFN treatment prevents DOX-induced pathology in mouse hearts

Freshly excised hearts from mice treated with DOX or with SFN ± DOX and from control mice were prepared for histological analysis as described in the Methods. Blue arrow indicates myofiber vacuolization; black arrow indicates myofibrillar disruption; and the star shows fibrosis. Bar = 50 μm.

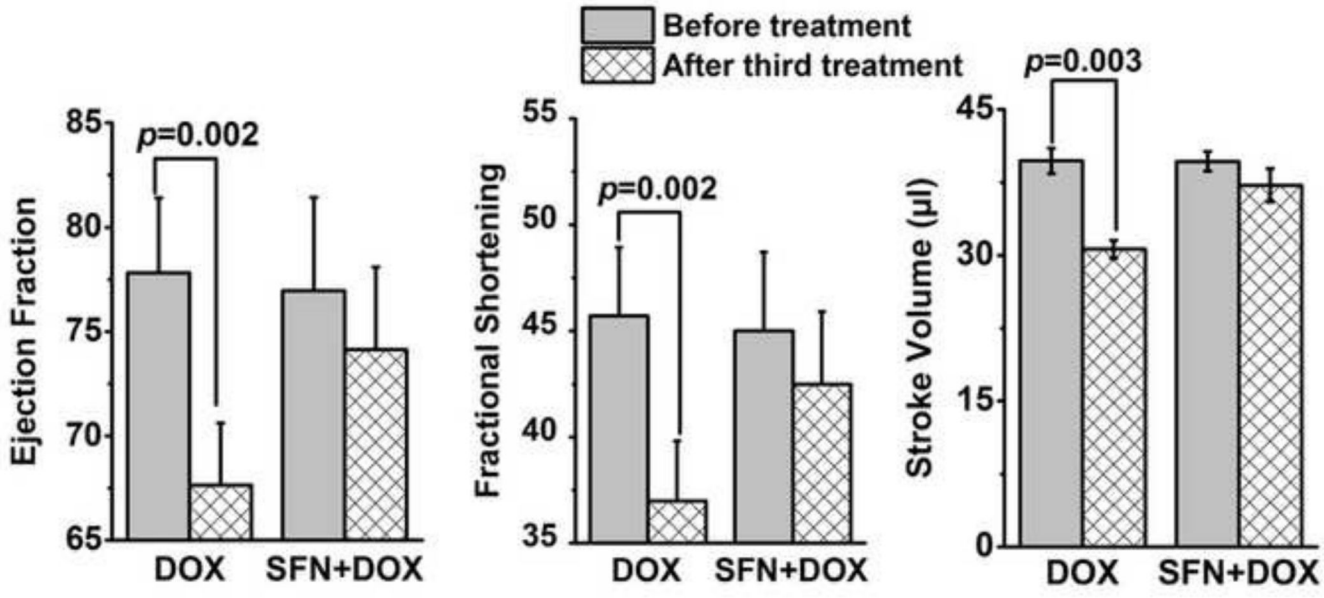

Figure 5. SFN treatment prevents DOX-induced cardiomyopathy in 129/sv mice

Adult mice were treated with DOX or SFN+DOX as described in the Materials and methods. Cardiac function was assessed before treatment and after the third DOX treatment (n = 12).

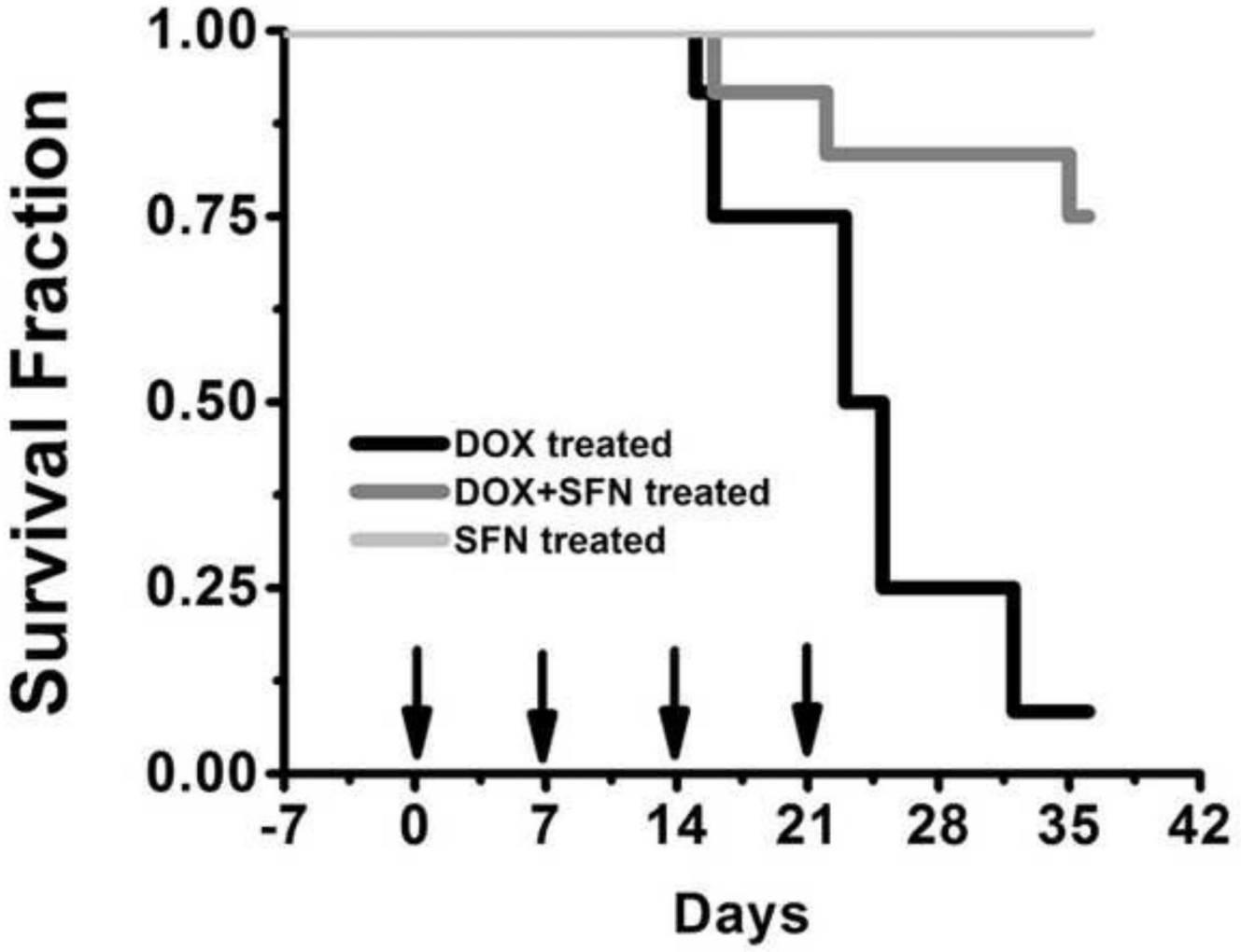

Figure 6. SFN treatment protects mice from DOX-induced toxicity

Mice were treated with i) DOX (total of 20 mg/kg i.p. for 4 weeks; arrows), ii) SFN (4 mg/kg s.c.; 5 days/week for 5 weeks) or iii) SFN+DOX. Survival for SFN+DOX- or SFN-treated mice was significantly higher than for DOX-treated mice (p=0.03, n = 12).

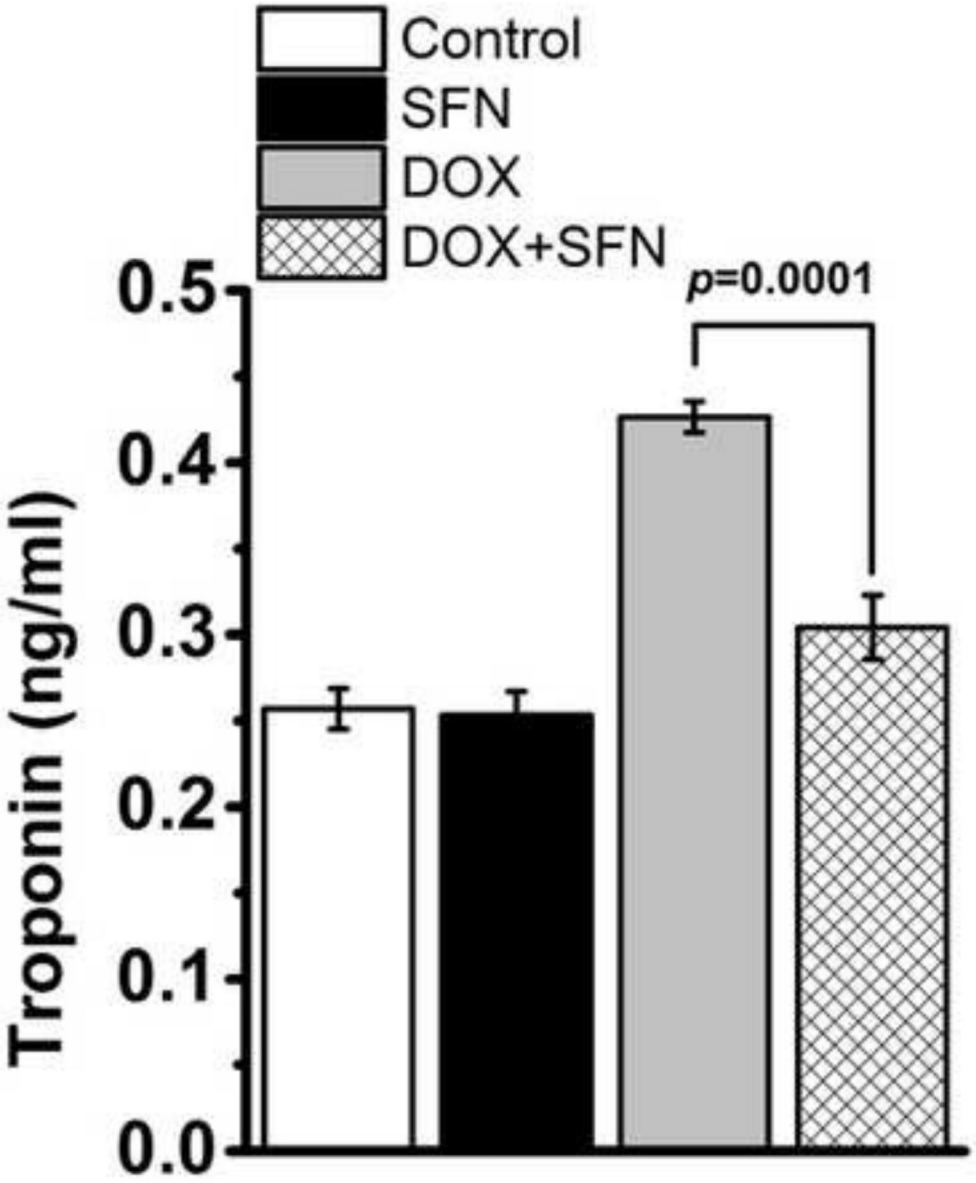

Figure 7. SFN treatment reduces cTnI release

cTnI levels were measured in plasma taken two days after the third DOX injection from mice treated with metronomic DOX +/− SFN or SFN as described in the Materials and methods. Data represent the means ± SD (n = 4).

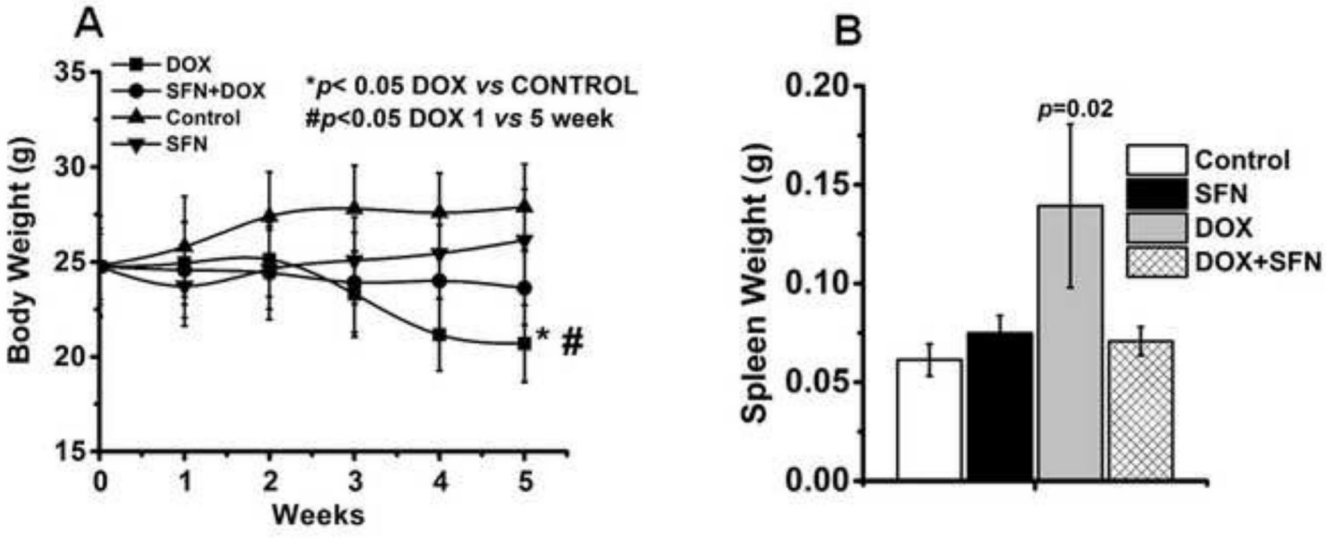

Figure 8.

A. Changes in body weight during the treatment with DOX, SFN+DOX, SFN or control. Data (collected as described in the Methods) represent the mean ± SD of gram body weight (n=12). B. Changes in spleen weight at the end of different treatments. Data represent the mean ± SD of gram spleen weight (n=12).

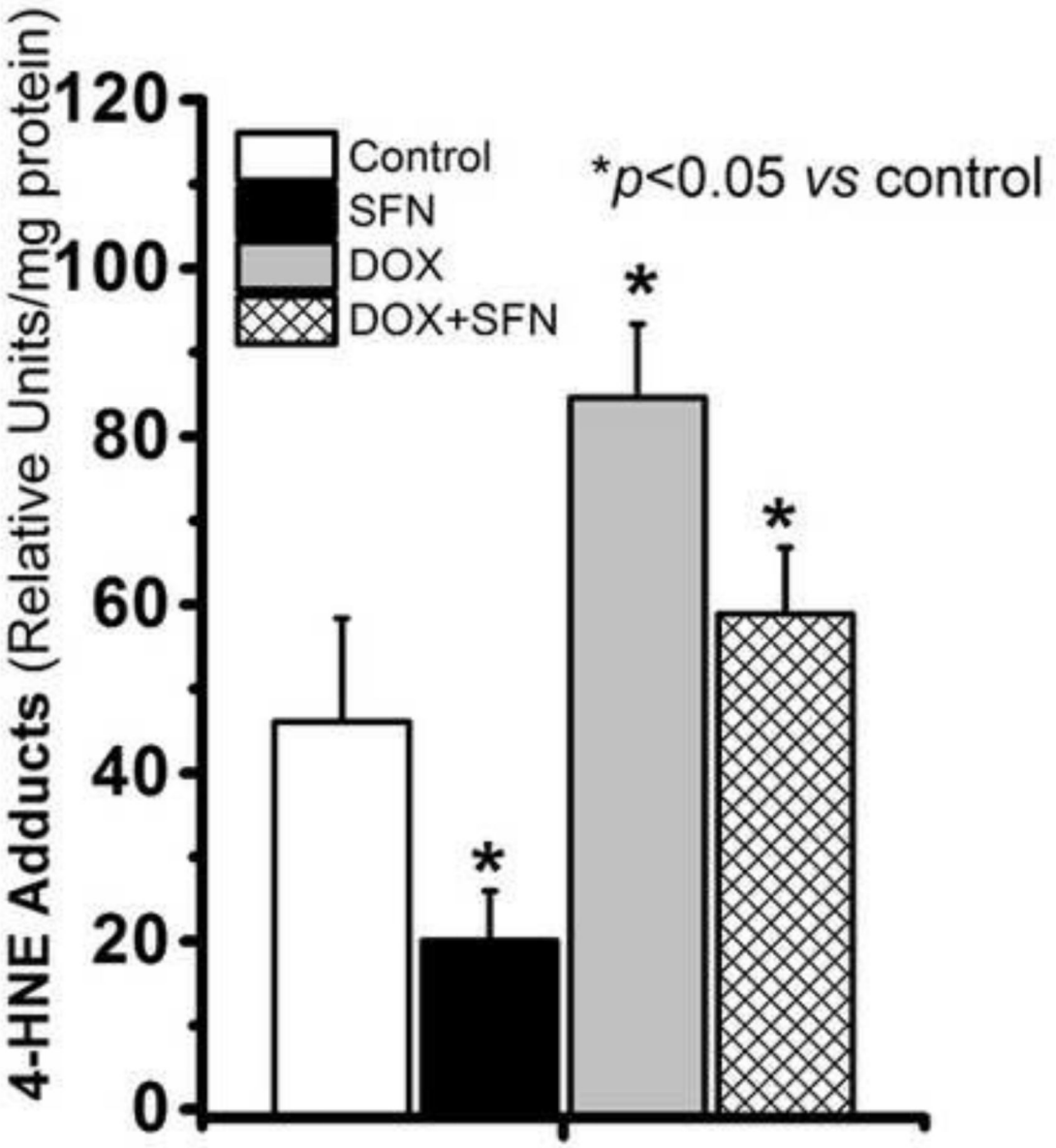

Figure 9. Total 4-HNE-protein adduct levels in hearts of mice treated with DOX, SFN+DOX, SFN or vehicle

Isolated cardiac tissue was homogenized and assayed for 4-HNE adducts as described in the Materials and methods. Data shown are means ± SD of triplicate measurements on homogenates (n = 4).

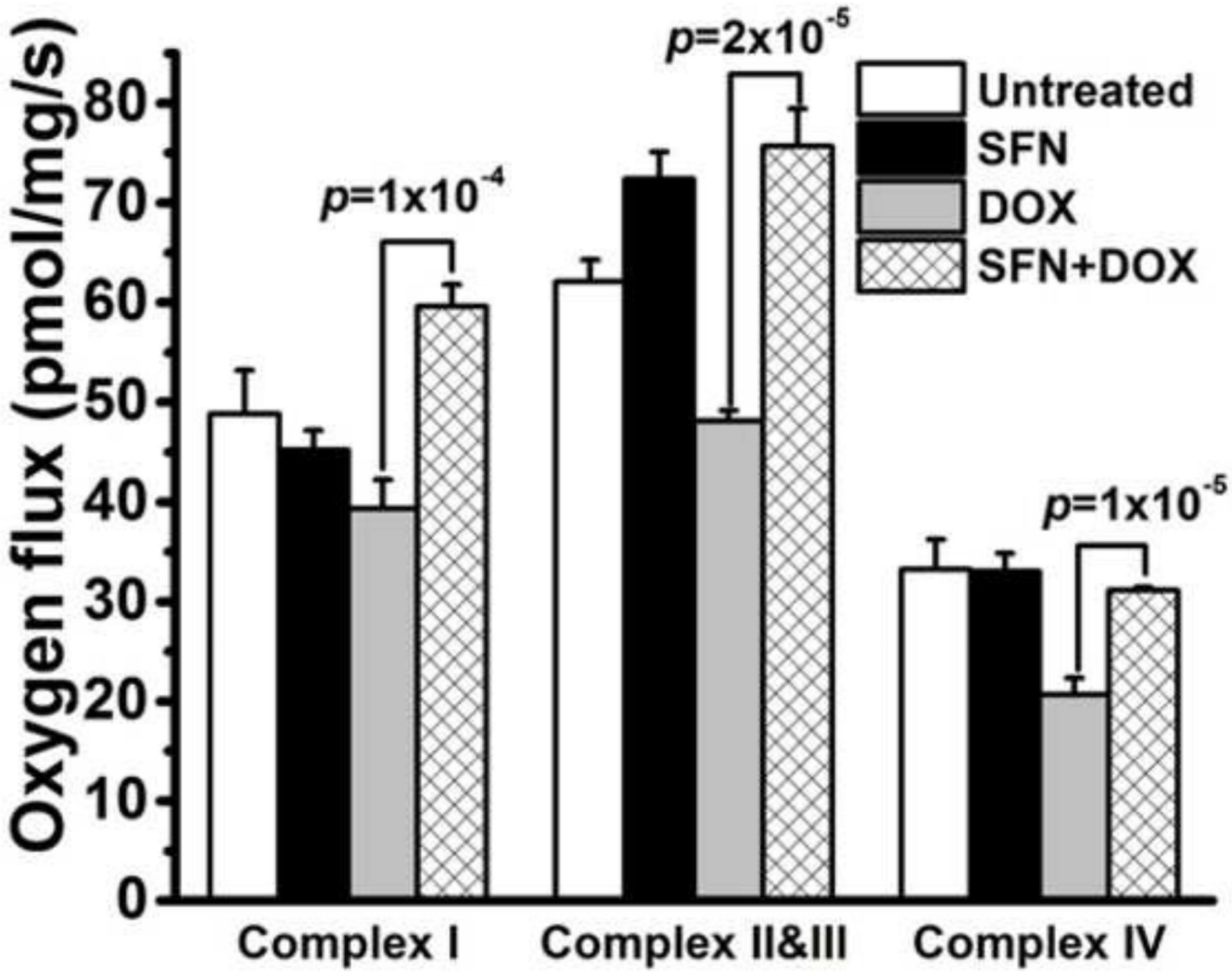

Figure 10. SFN improves ETC function during DOX treatment

Respiration status of complexes I, II+III, and IV of the ETC was evaluated in fresh heart biopsies using the HRR technique as described in the Materials and methods. According to oxygen flux measures, co-treatment of mice with SFN+DOX significantly improved complex I, II+III and IV respiration compared to mice treated only with DOX. Each bar represents mean ± SD (n = 8).

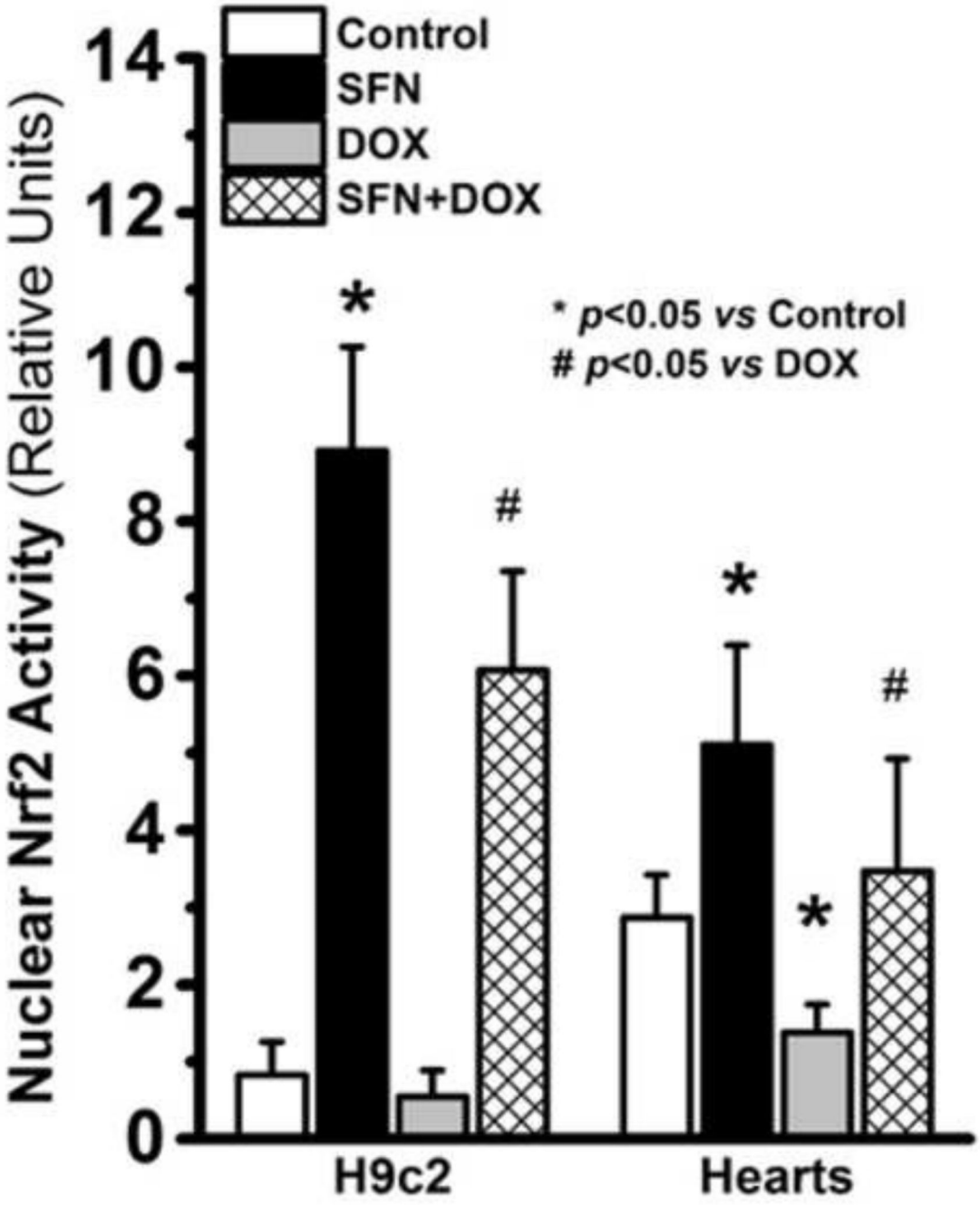

Figure 11. Quantitation of active nuclear Nrf2 from H9c2 cells or hearts of control and treated mice

Nrf2 binding activity was measured by ELISA in nuclear extracts from H9c2 cells or from the LV portion of control and treated mice. The nuclear fractions from each heart and from H9c2 cells were assayed separately in duplicates (n = 4).

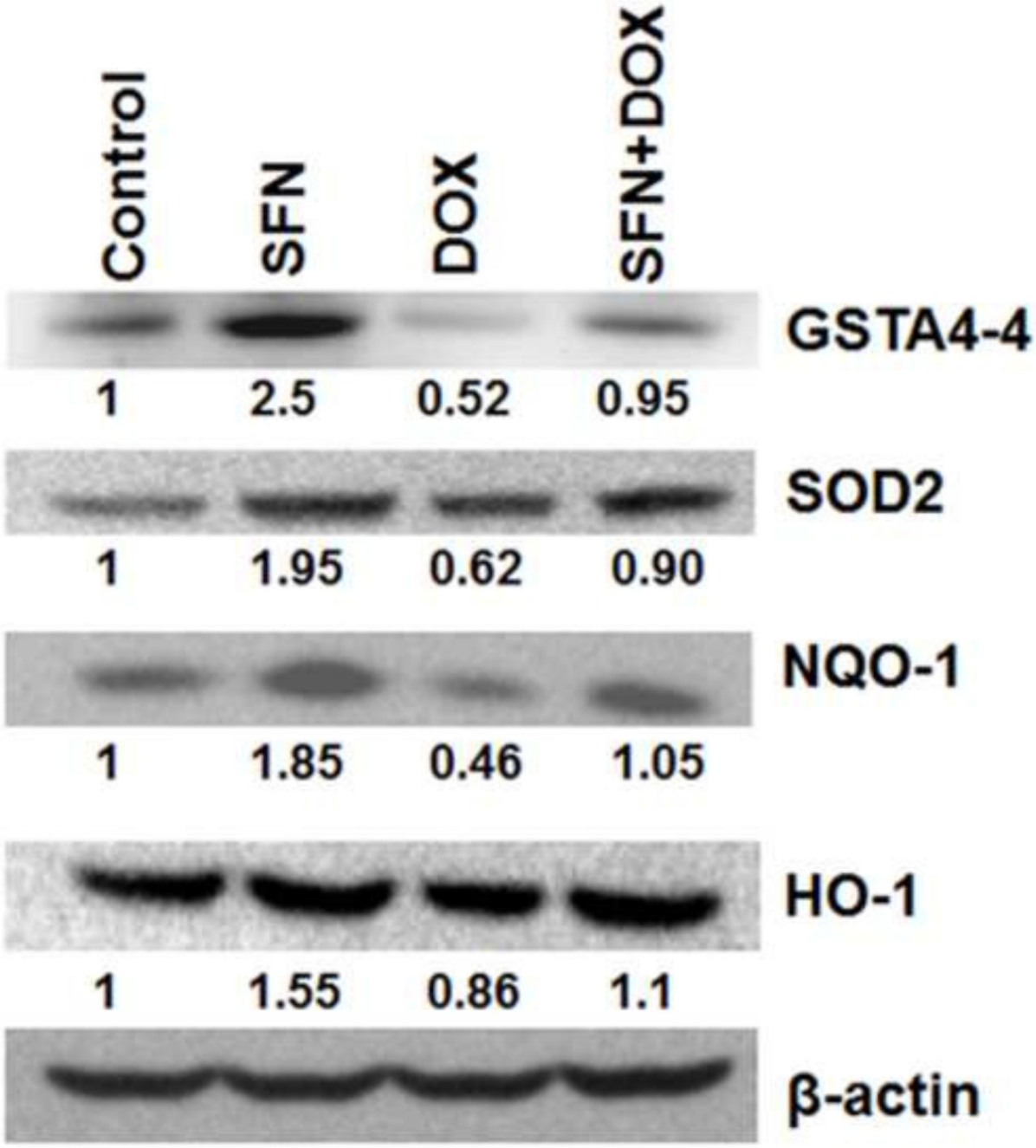

Figure 12. SFN treatment restores antioxidant/anti-electrophile enzyme expression from DOX-induced repression

Heart homogenates from vehicle-, SFN-, DOX- and SFN+DOX-treated mice were examined by western blot analysis for levels of NQO-1, HO-1, SOD2, GSTA4-4 and β-actin (n=4–6 per group). Grayscale values of the GSTA4-4, SOD2, NQO-1 and HO-1 bands, normalized with β-actin using ImageJ software (developed by NIH) are shown under the corresponding bands to indicate the relative expression level of proteins in a representative western blot.

Table 1

Microscopic findings in myocardia from control, SFN, DOX+/−SFN treated mice

	Cytoplasmic vacuolization	Myofibrillar disruption	Fibrosis
Control	0/4	0/4	0/4
SFN	0/4	0/4	0/4
DOX	8/8 (2.6)	8/8 (2.5)	3/8 (1)
DOX+SFN	2/8 (1)	3/8 (1)	0/8

Myocardial tissue was examined for cytoplasmic and myofibrillar changes and fibrosis. Data are presented as number of animals affected/number of animals examined; average severity (ranging from 1 to 3, least to most severe) of affected animals is indicated in parentheses. Microscopic examination was determined by a pathologist using scoring criteria described in the Materials and methods.

Table 2

Relative levels of Nrf2 target gene transcripts from control and treated mice

	CONTROL	SFN	DOX	DOX+SFN
Cat	0.92±0.10	2.71±0.41*	0.28±0.03*	0.82±0.06
Sod1	3.96±0.26	7.49±0.53*	1.08±0.36*	3.22±0.31
Sod2	3.58±0.17	12.40±0.83*	1.31 ±0.17*	4.39±0.12
Pxdn	0.32±0.08	0.31 ±0.16	0.33±0.09	0.29±0.14
Gpx1	1.00±0.07	1.77±0.18*	0.41±0.15*	0.83±0.53
Gpx4	2.43±0.54	2.88±0.86	2.22±0.39	1.91 ±0.49
Txnrd1	0.02±0.01	0.02±0.01	0.03±0.01	0.03±0.01
HO-1	0.13±0.06	0.36±0.05*	0.06±0.03*	0.18±0.02
NQO1	0.36±0.03	1.07±0.20*	0.17±0.05*	0.30±0.03
Gsta1+2	0.03±0.01	0.05±0.02	0.05±0.01	0.02±0.01
Gsta3	0.07±0.02	0.08±0.03	0.06±0.01	0.06±0.05
Gsta4	1.90±0.81	4.53±1.18*	1.08±0.14*	2.09±0.48
Gstm1	0.65±0.24	0.76±0.30	1.18±0.31*	0.83±0.25
Aor	0.02±0.01	0.01±0.01	0.03±0.01	0.01±0.001
Akr3	2.47±0.16	1.62±0.42	0.59±0.06*	0.89±0.16*
Akr8	0.38±0.11	0.13±0.08*	0.10±0.05*	0.23±0.19
Gclc	0.13±0.02	0.17±0.01 *	0.06±0.02*	0.10±0.02
Gclm	0.06±0.01	0.05±0.01	0.04±0.02	0.05±0.03

Levels of Nrf2-regulated transcripts encoding antioxidant and anti-electrophile enzymes, and enzymes involved in glutathione biosynthesis were measured by qRT-PCR in hearts of control and treated animals. Gene expression levels were normalized to the S3 ribosomal protein transcript and calculated as described in the Materials and methods. Asterisks denote statistically significant differences ($p < 0.05$; n = 5) between control and treated groups of animals, compared pairwise.